CrossMark

ARTICLE

Structural setting of Fimiston- and Oroya-style pyrite-telluride-gold lodes, Paringa South mine, Golden Mile, Kalgoorlie: 1. Shear zone systems, porphyry dykes and deposit-scale alteration zones

Andreas G. Mueller[1]

Abstract The Golden Mile in the 2.7 Ga Eastern Goldfields Province of the Yilgarn Craton, Western Australia, has produced 385 million tonnes of ore at a head grade of 5.23 g/t gold (1893–2016). Gold-pyrite ore bodies (Fimiston Lodes) trace kilometre-scale shear zone systems centred on the D2 Golden Mile Fault, one of three northwest striking sinistral strike-slip faults segmenting upright D1 folds. The Fimiston shear zones formed as D2a Riedel systems in greenschist-facies (actinolite-albite) tholeiitic rocks, the 700-m-thick Golden Mile Dolerite (GMD) sill and the Paringa Basalt (PB), during left-lateral displacement of up to 12 km on the D2 master faults. Pre-mineralisation granodiorite dykes were emplaced into the D2 shear zones at 2674 ± 6 Ma, and syn-mineralisation diorite porphyries at 2663 ± 11 Ma. The widespread infiltration of hydrothermal fluid generated chlorite-calcite and muscovite-ankerite alteration in the Golden Mile, and paragonite-ankerite-chloritoid alteration southeast of the deposit. Fluid infiltration reactivated the D2 shear zones causing post-porphyry displacement of up to 30 m at principal Fimiston Lodes moving the southwest block down and southeast along lines pitching 20°SE. D3 reverse faulting at the southwest dipping GMD-PB contact of the D1 Kalgoorlie Anticline formed the 1.3-km-long Oroya Shoot during late gold-telluride mineralisation. Syn-mineralisation D3a reverse faulting alternated with periods of sinistral strike-slip (D2c) until ENE-WSW shortening prevailed and was accommodated by barren D3b thrusts. North-striking D4 strike-slip faults of up to 2 km dextral displacement crosscut the Fimiston Lodes and the barren thrusts, and control gold-pyrite quartz vein ore at Mt. Charlotte (2651 ± 9 Ma).

Keywords Kalgoorlie · Riedel shears · Thrust faults · Sericite · Gold

Editorial handling: S. Hagemann

✉ Andreas G. Mueller
   andreasm@iinet.net.au

[1] Centre for Exploration Targeting, School of Earth and Environment, The University of Western Australia, 35 Stirling Highway, Perth, Western Australia 6001, Australia
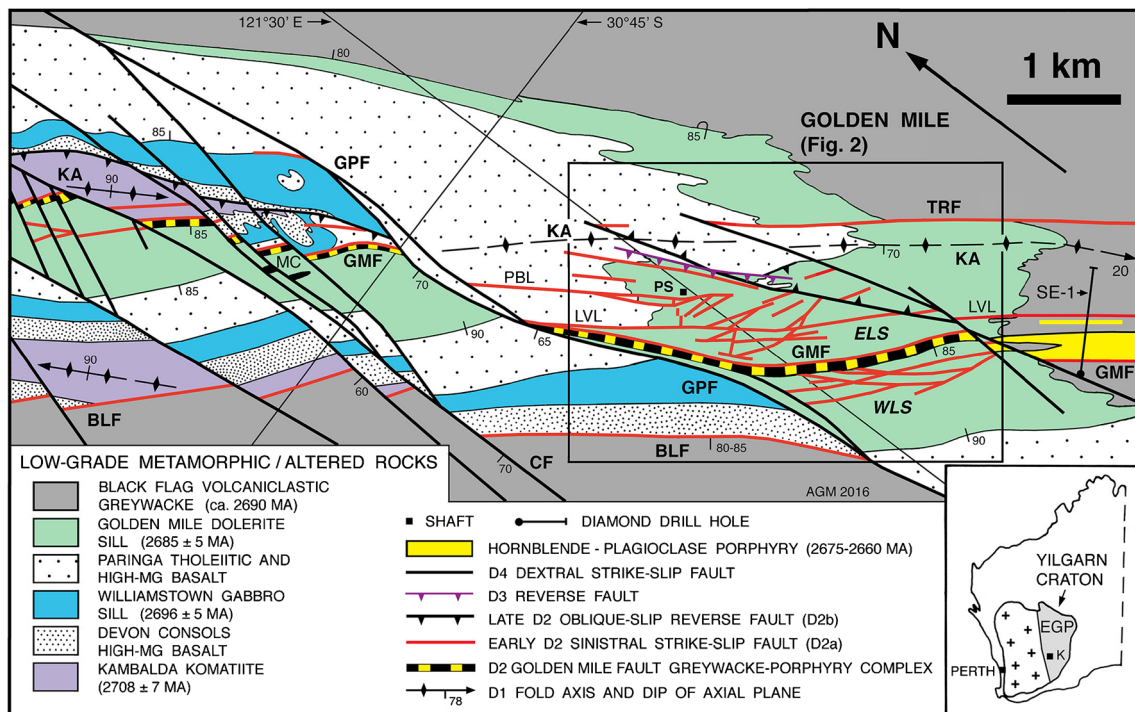
Introduction

The Kalgoorlie mining district, located in the Eastern Goldfields fold belt of the Archean Yilgarn Craton at 30° 47′ south latitude and 121° 29′ east longitude, comprises two world-class gold deposits: Mt. Charlotte in the northwest (148 t Au to 2016) and the Golden Mile in the southeast (1731 t Au). Production from the Golden Mile is subdivided into underground (1893–1992, 105.6 Mt at 13.1 g/t Au mill head grade) and open pit (1984–2016, 279 Mt at 2.26 g/t Au). The average recovery of gold from the refractory pyrite-telluride ore is estimated at 86% (App. 1; Electronic Supplementary Material). Tellurides account for 15–20% of the total gold. In contrast, they are insignificant (<1%) in the Mt. Charlotte deposit (Clout et al. 1990). The Golden Mile covers an area 4.5 km long and 1.1 km wide, and consists of hundreds of mineralised shear zones centred on the district-scale Golden Mile Fault (Fig. 1). The largest ore body, the Horseshoe No. 4 Lode, was mined over a strike of 1800 m and to 1160 m vertical depth (Travis et al. 1971). Traditionally, the pyrite-rich ore bodies located in steeply dipping shear zones are termed Fimiston Lodes, whereas late telluride-rich ore is distinguished as Oroya-style mineralisation (e.g.

🖄 Springer

Fig. 1 Structural map of the Kalgoorlie district (modified from Mueller 2015). Metamorphic and metasomatic rocks are not differentiated. The zircon U-Pb ages of the units dated are listed (see Fletcher et al. 2001; Mueller et al. 2016; this issue). The structures are ordered according to the time of formation (D1 to D4), and not according to the time of gold mineralisation. The Boulder-Lefroy (BLF), Golden Mile (GMF) and Trafalgar (TRF) sinistral strike-slip faults (D2a) displace the upright D1 Kalgoorlie Anticline (KA) and Syncline (KS). The Golden Mile master fault separates the Western from the Eastern Lode System (WLS, ELS). Note the Lake View Lode (LVL) and Paringa B-Lode (PBL), the Paringa South (PS) shaft and the porphyry complex intersected by South End drill hole SE-1. Dextral D4 shear zones such as the Golden Pike (GPF) and Charlotte Faults (CF) control quartz-vein ore bodies mined at Mt. Charlotte (MC). The coordinates are latitude and longitude. The *inset map* of Western Australia shows the Eastern Goldfields Province (EGP) in the Yilgarn Craton, and the cities of Perth and Kalgoorlie (K)

Hagemann and Cassidy 2000). The Paringa South underground mine in the northwest part of the Golden Mile (Fig. 1) produced 4.0 Mt at 19.4 g/t Au (1893–1967), and 0.626 Mt at 4.36 g/t Au + 1.05 g/t Ag (recovered grade) from 1983 until closure in 1987 during the expansion of the open pit.

Documentation of the lode system progressed slowly. The basic structure did not emerge until Stillwell (1929) compiled geologic plans and sections across lease boundaries. Comprehensive studies of shear zones in parts of the Golden Mile include those of Larcombe (1913), Feldtmann (1928), Finucane (1941, 1948, 1964), Tomich (1952, 1959), and Wells (1964). Systematic mapping ceased with the closure of all underground operations in 1992. The structural framework of the deposit, constrained in time by porphyry emplacement and U-Pb chronology, is reviewed first followed by a description of the kilometre-scale alteration zones enclosing the lodes. These data are integrated with structural mapping on levels of the Paringa South shaft, and with reconnaissance mapping in the adjacent North Kalgurli mine. Crosscutting relationships and U-Pb ages indicate that the lodes formed about 10 million years after the emplacement of granodiorite dykes into post-folding strike-slip faults. Gold mineralisation

took place in a regime of alternating sinistral strike-slip and reverse faulting during the transition to regional shortening in the fold belt. The deformation sequence established in this study provides the basis for the distinction of mineralisation stages in lodes of the Paringa South mine described in subsequent contributions focussed on petrography, geochemistry, mineralogy and the PTX conditions of ore formation (Parts 2 and 3).

Methods and terminology

Structural mapping on levels 4, 7 and 11 of the Paringa South shaft was carried out by the author in 1986 and 1987 on survey plans (1:1000) provided by Gold Resources Pty. Ltd., the company operating the underground mine. The Paringa South level 7 plan also covers part of the adjacent North Kalgurli mine as the two former companies shared their data to join shaft levels matched in elevation. The plans and sections provided showed the mine workings and stopes, parts of lodes and faults, and gold grade ± lithology at drill holes. These scattered historic data were integrated with the results of own mapping to reconstruct the folded contact Golden Mile

Dolerite-Paringa Basalt, and the positions of lodes and faults on the three structural maps and on the Paringa South shaft cross section presented below. The location of stopes in the Oroya Shoot and of the Brownhill East Lode on level 4 is according to Lungan (1986). Coordinates are in the metric mine grid and datum (Mt. Charlotte water tank = 421.2 m asl) applied across the Golden Mile. The pre-mining surface is approximately 385 m above sea level. The traditional names of shafts, lodes and faults are retained to allow correlation with older literature.

Most lodes are composed of brittle fault-fill and breccia veins (e.g. Robert and Poulsen 2001), whereas many faults and some lodes consist of ductile S-C mylonite (e.g. Lister and Snoke 1984). Ladder veins are planar extension veins oriented perpendicular to the walls of competent zones in the lodes. They define an opening vector parallel to the movement vector (Robert and Poulsen 2001). The Fimiston Lodes are classified according to the strike angle they form with the Golden Mile master fault: principal displacement zones (PDZ, parallel), Riedel shears (R, 15–20° anticlockwise), conjugate Riedel shears (R′, 60–75° clockwise), secondary synthetic shears (P, 15–20° clockwise), and extensional faults or veins (T, 45° anticlockwise), a system generated in initially isotropic rocks by simple shear (e.g. Davis et al. 2012).

The mineralogy of altered rocks was determined by X-ray diffraction (XRD) using the Philips PW1700 powder diffractometer and graphical software at the University of Western Australia. The term "sericite" is used for fine-grained white mica, if both muscovite and paragonite are present, and the term "silica" for chert-like replacement quartz and chalcedony. Whole-rock samples of porphyry dykes were analysed for major oxides and trace elements by X-ray fluorescence (XRF) and inductively coupled plasma torch mass spectrometry (ICP-MS). Details are given in the footnotes of the data table. The sensitive high mass resolution ion microprobe (SHRIMP) and thermal ionisation mass spectrometry (TIMS) U-Pb ages are quoted at the 95% confidence level. All are zircon ages except where stated otherwise.

Greenstone-belt stratigraphy

The regional geology of the Yilgarn Craton is reviewed in Witt et al. (2017; this issue), and the tectonic setting of the gold-rich south Kalgoorlie Terrane in Mueller et al. (2016; this issue). This contribution is focussed on the structure of the Golden Mile deposit in the Kalgoorlie mining district.

The stratigraphic succession at Kalgoorlie includes, from the oldest to the youngest unit (nomenclature: Swager et al. 1995), the Kambalda komatiite flows, the Devon Consols magnesian pillow basalt, the Paringa pillow basalt comprising a lower magnesian (7–14 wt.% MgO; Bateman et al. 2001a) and an upper tholeiitic unit (2.5–4.2% MgO) and the Black

Flag greywacke (Fig. 1). The pillow basalts are subdivided by black shale marker beds: the 1–10 m thick Kapai Slate separating the Devon Consols and Paringa units (Travis et al. 1971), and an unnamed bed separating the lower and upper Paringa basalts (Tomich 1959). Two mafic sills are emplaced into the succession: the 150–300 m thick Williamstown gabbro above the Kapai Slate and the 600–750 m thick Golden Mile Dolerite (GMD) at the contact Paringa Basalt-Black Flag greywacke. The Kambalda Komatiite is dated at 2708 ± 7 Ma (Nelson 1997), the Williamstown gabbro at 2696 ± 5 Ma (Fletcher et al. 2001) and the Golden Mile Dolerite at 2685 ± 5 Ma (Tripp 2013). The succession is metamorphosed to the actinolite-albite greenschist facies (Travis et al. 1971), and overprinted by the kilometre-scale hydrothermal alteration zones described below.

Golden Mile Dolerite and Paringa Basalt

The GMD sill and the upper part of the Paringa Basalt are the principal host rocks of the Golden Mile lodes. The sill has been subdivided into ten units on the basis of geochemistry, texture and Fe-Ti oxide morphology (Travis et al. 1971). The variolitic units 1 and 10 represent the lower and upper chilled margins, units 2 and 3 the basal pyroxene cumulate zone and units 4, 5 and 9 ophitic quartz gabbro. These units formed by differentiation of the initial pulse of tholeiitic magma. The central units 6 to 8 differ due to the abundance of titanomagnetite and ilmenite (14–18 wt.% $FeO + Fe_2O_3$; 1.7–3.0% TiO_2). Unit 8 is characterised by granophyric quartz-albite intergrowth. The three central units are interpreted to result from the late injection of fractionated tholeiitic magma. The ten units persist across the district over a strike of 13 km, and the central iron-rich ones lens out 8 km southeast of the Golden Mile (Travis et al. 1971). The sill thins to less than 200 m on the northeast limb of the Kalgoorlie Anticline (Fig. 1), and changes to the Eureka petrographic facies (Bateman et al. 2001a). The upper Paringa pillow basalt, about 150 m thick above the marker black shale, also has a high-titanium tholeiitic composition (1.2–1.8% TiO_2; Bateman et al. 2001a). Phenocrysts of plagioclase are common but Ti-magnetite is absent.

District-scale structures

The structural framework of the Golden Mile is reviewed below based on work in Stillwell (1929), Gustafson and Miller (1937), Woodall (1965), Travis et al. (1971), Keats (1987), Mueller et al. (1988), Clout et al. (1990), Bateman et al. (2001b), Gauthier et al. (2004) and Mueller et al. (2016; this issue). The structures are described in the sequence of relative timing (D1 to D4) constrained by U-Pb ages. Structures related to the same deformation event but separated in time are

distinguished using lowercase letters (e.g. D2a to D2c). Gold-pyrite-telluride mineralisation in the Golden Mile took place during D2c and D3a faulting, mostly confined to reactivated D2a and D2b shear zones.

Regional folds (D1)

The Kalgoorlie Anticline and Syncline, outlined by the Golden Mile Dolerite (Fig. 1), are upright tight folds plunging 20°SE (Travis et al. 1971). The northeast limb of the Kalgoorlie Anticline is sub-vertical (80–90°NE), and the southwest limb dips 40–50°SW. Both limbs define an axial plane oriented N35–40°W/65–75°SW. A weak foliation caused by aligned plagioclase and pyroxene pseudomorphs in chloritic GMD (Ion 1982; Fotios 1983) is interpreted as an axial-plane D1 metamorphic fabric. The subsidiary Brownhill Syncline on the southwest limb of the main anticline (Fig. 2) plunges at shallow angles southeast but diminishes in amplitude and fades 300 m below surface (Woodall 1965).

A sheared wedge of carbonaceous Black Flag greywacke marks the core of the Kalgoorlie Syncline (Figs. 2 and 3). The Golden Mile Fault forms the northeast contact. In the southwest, the greywacke is in conformable contact with GMD Unit 10 (Travis et al. 1971). Another fault-bounded greywacke syncline occurs adjacent to the Lake View Lode at the Lake View South shaft (Fig. 2) closing about 100 m below surface (Gustafson and Miller 1937; Gauthier et al. 2004). The D1 folding took place after the emplacement of the GMD sill at 2685 ± 5 Ma (Tripp 2013).

Early sinistral strike-slip faults (D2a)

The D1 folds are displaced by D2a transcurrent faults, which strike northwest and dip 80–85°SW: the Boulder Lefroy Fault southwest of the Golden Mile, the central Golden Mile Fault (GMF), and the Trafalgar Fault to the northeast (Figs. 1 and 2). The steeply southwest dipping shear zones of the Western and Eastern Lode Systems, interpreted as sinistral Riedel-type networks (Mueller et al. 1988), are centred on the Golden Mile master fault and bounded by the Boulder Lefroy and Trafalgar Faults. The Trafalgar Fault, intersected by drill holes southeast of the Golden Mile (Fig. 2), offsets the northeast limb of the Kalgoorlie Anticline 660 m in a sinistral sense (Woodall 1965; Travis et al. 1971). The amount of displacement on the GMF is not constrained.

The Boulder Lefroy-Golden Mile fault system extends 30 km southeast to the Hampton-Boulder gold deposit, where the Boulder Lefroy Fault transects an isoclinal D1 anticline and offsets two vertical meta-gabbro sills 11–12 km in a left-lateral sense. Most of the D2a sinistral movement took place before the emplacement of a granodiorite porphyry dyke at 2676 ± 7 Ma. The dyke is boudinaged but not dismembered

Fig. 2 Geologic map of the Golden Mile deposit at 300 m above sea level constructed using the gold grade plan in Bateman et al. (2001b), geologic maps (Stillwell 1929; Woodall 1965; Clout et al. 1990) and own data. The coordinates are metric mine grid. The structures are ordered according to the time of formation (D1 to D4), and not according to the time of gold mineralisation. The pattern of D2a Fimiston Lodes is slightly distorted due to D2b reverse faults not shown except for the Australia East Fault. The sericite (muscovite > paragonite)-ankerite alteration zone in Paringa Basalt merges with the paragonite-ankerite-chloritoid zone in Golden Mile Dolerite centred on the D2a Trafalgar Fault. Minerals: albite (ab), ankerite (ank), calcite (cal), chlorite (chl), dolomite (dol), epidote (ep), muscovite (ms), paragonite (pg). Shafts: Aberdare (ABD), Adelaide (AD), Boulder Main (BM), Chaffers (CH), Drysdale (DY), Edwards (ED), Golden Pike (GP), Iron Duke (ID), Judd (JD), Kalgurli (KL), Lake View Main (LV), Lake View South (LS), Lake View town site (LVT), North Kalgurli (NK), Paringa South (PS), Perseverance (PV), Pomeroy (PO), South Kalgurli (SK). Drill holes: Trafalgar TRF-1 to TRF-5. Eastern D2a/D3a lodes: B-Lode (B-L), Federal (FDL), Kelly (KEL), Lake View (LVL), Oroya Hanging Wall (OHW). Western D2a lodes: Horseshoe No. 1 (H1L), No. 2 (H2L), No. 3 (H3L), No. 4 (H4L), Morrison (MOR). D2 to D4 faults: Adelaide (ADF), Australia East (AEF), Boulder Lefroy (BLF), Golden Mile (GMF), Golden Pike (GPF), Hannan Star (HSF), Trafalgar (TRF). D1 folds: Brownhill Syncline (BHS), Kalgoorlie Anticline (KLA), Kalgoorlie Syncline (KLS)

like the D1 anticline (Figs. 2 and 4 in Mueller et al. 2016; this issue).

At Kalgoorlie, granodiorite dykes are abundant in the carbonaceous schist marking the D2a Golden Mile Fault (Gustafson and Miller 1937). They record U-Pb ages of 2671 ± 10 Ma in the Golden Mile (Vielreicher et al. 2010) and 2673 ± 11 Ma at Mt. Charlotte (Yeats et al. 1999; error adjusted to account for the low number of analyses, $n = 5$). Another granodiorite dyke, emplaced into Golden Mile Dolerite adjacent to the GMF, has been dated at 2674 ± 6 Ma (Kent and McDougall 1995).

Late sinistral reverse faults (D2b)

The Australia East Fault (AEF in Fig. 2) represents a system of oblique-slip reverse faults oriented N20°W/65–80°NE, which are abundant northeast but sparse southwest of the Golden Mile Fault. The AEF has an apparent reverse offset of 180 m at GMD Unit 8 (Fig. 3). Structural relationships indicate that the D2b faults offset D2a shear zones (Fig. 4a) but that both formed prior to the intrusion of granodiorite dykes at 2674 ± 6 Ma. The granodiorite porphyry emplaced into the D2a shear zone controlling the Lake View Lode, for example, dips southwest on the lower levels of the South Kalgurli shaft but changes in dip at D2b faults on the upper levels (Fig. 4a).

The original movement on D2b faults prior to D2c reactivation (see below) was probably reverse oblique-slip east block up and north. Tomich (1952) determined a sinistral-reverse offset of 32 m at a D2b fault exposed on the Lake View shaft −550 m level by correlating the pitch-line intersection points of D2a shear zones on both sides of the fault plane. Fotios (1983) obtained 150 m of movement along a line
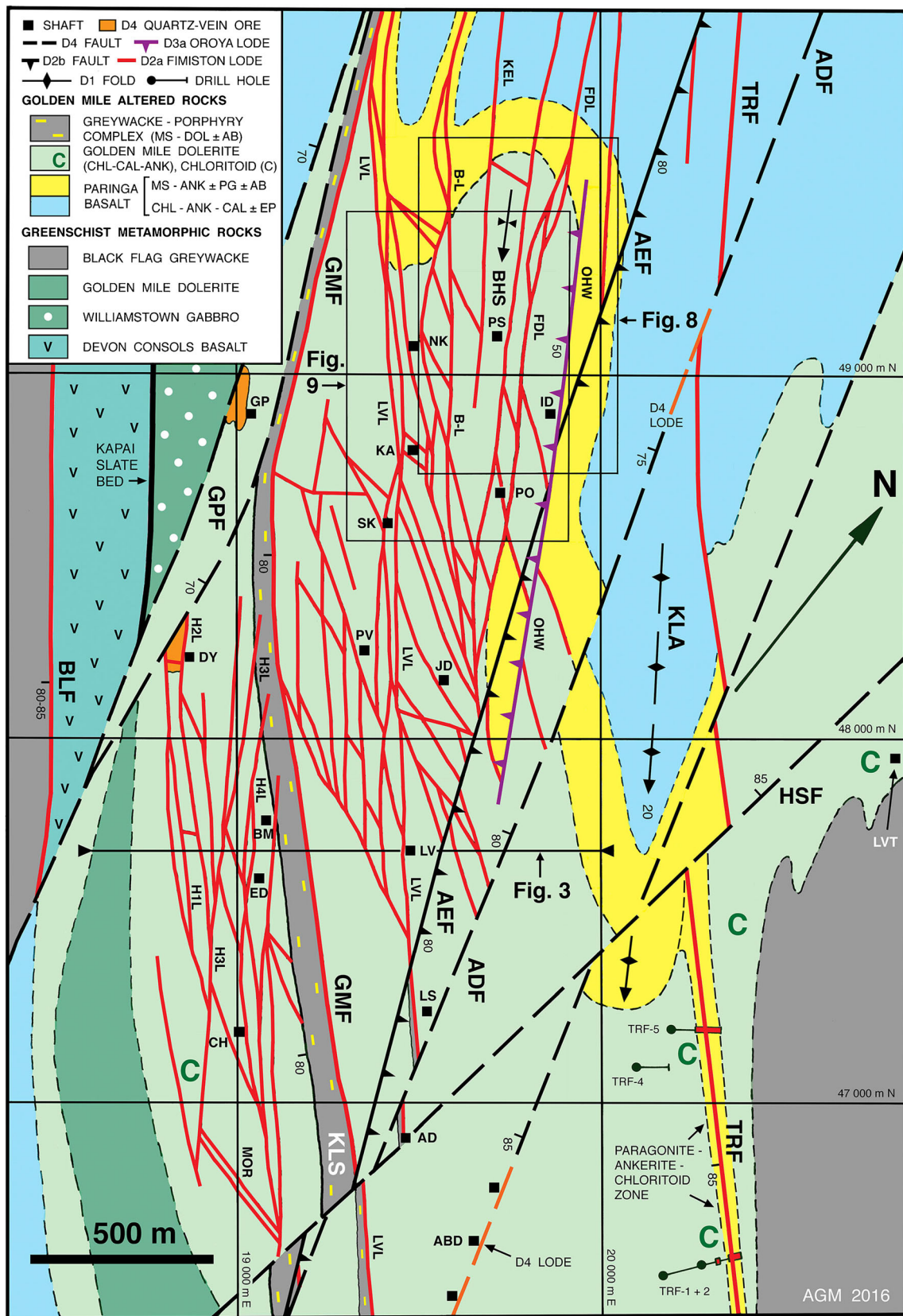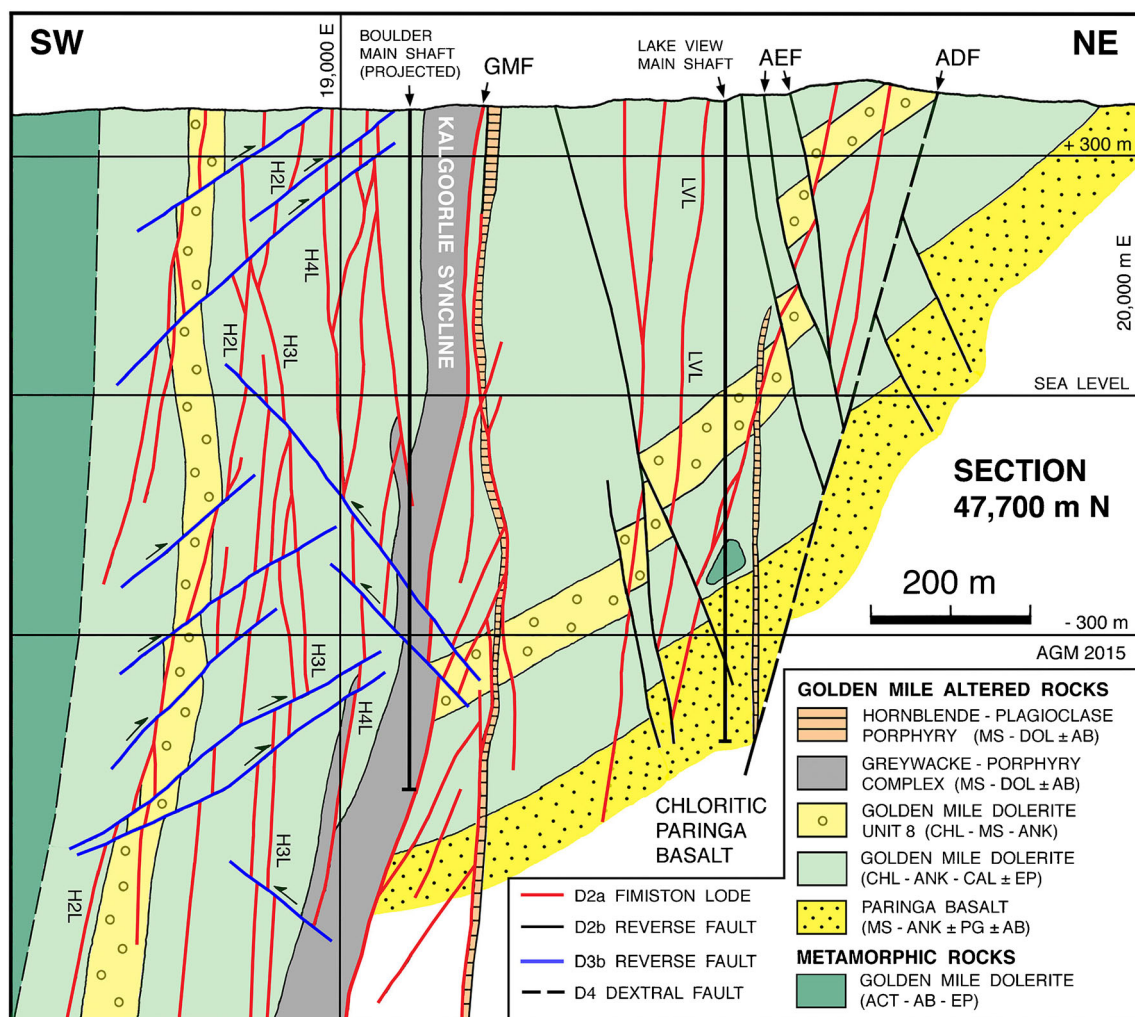
Fig. 3 Cross section through the D1 Kalgoorlie Syncline, the D2a Golden Mile Fault (GMF) and the D2a Fimiston Lodes at 47,700 m grid north (modified from Mueller et al. 1988). The structures are ordered according to the time of formation (D1 to D4), and not according to the time of gold mineralisation. The D3b reverse faults are barren. The transition from chlorite-calcite altered to metamorphic Golden Mile Dolerite and from sericite-ankerite to chlorite-calcite altered Paringa Basalt is gradual. Minerals: actinolite (act), albite (ab), ankerite (ank), calcite (cal), chlorite (chl), dolomite (dol), epidote (ep), muscovite (ms), paragonite (pg). D2a Fimiston Lodes: Horseshoe No. 2 (H2L), No. 3 (H3L), No. 4 (H4L), Lake View (LVL). Faults: D2b Australia East (AEF), D4 Adelaide (ADF)

inclined 60°S on another D2b fault surface using the same method and the pitch lines of the GMD Unit 6/7 contact and a D2a shear zone.

Post-porphyry sinistral strike-slip (D2c)

The granodiorite porphyry in the D2a Boulder Lefroy Fault at the Hampton-Boulder deposit was boudinaged, overprinted by sericite-dolomite-pyrite alteration and crosscut by gold-bearing fault-fill veins subsequent to emplacement at 2676 ± 7 Ma. The steep plunge of the boudin axes indicates post-porphyry, syn-mineralisation strike-slip (D2c) along a line pitching 21°SSE consistent with a small normal component moving the southwest block down and south (Mueller et al. 2016; this issue).

In the Golden Mile, D2b faults of the Australia East system terminate Fimiston Lodes controlled by D2a shear zones but are also mineralised in places (Fig. 4a), indicating that fluid infiltration reactivated both. Syn-mineralisation movements offset not only the granodiorite dykes dated at 2674 ± 6 Ma but also a younger generation of diorite dykes (Fig. 4b). Dyke offsets of 30 m or less (Tomich 1952; Mueller et al. 1988) show that the reactivation was small scale compared to the kilometre-scale movement during D2a faulting. Published evidence for syn-mineralisation sinistral strike-slip (D2c) includes slickenlines pitching 15–30°S on D2b faults (Gustafson and Miller 1937), and the geometry of gold-telluride fault-fill veins within the D2a Golden Mile Fault at Mt. Charlotte (Mueller 2015). The subdivision into D2a and D2b faults is retained in all figures of this study, as they differ in orientation and formed at
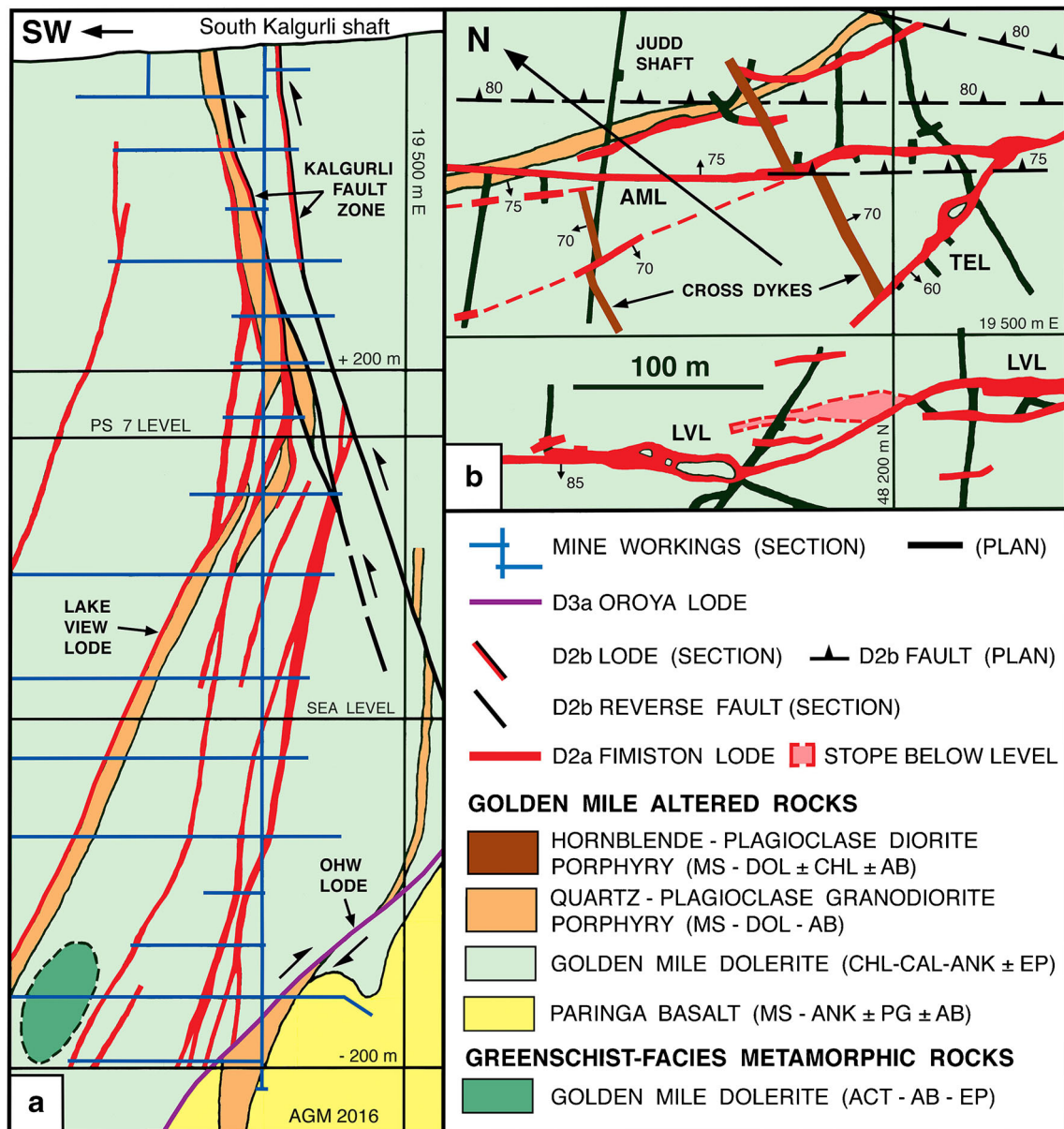
Fig. 4 Structural relations between faults and porphyry dykes, Eastern Lode System, Golden Mile, Kalgoorlie. The structures are ordered according to the time of formation (D2a to D3a), and not according to the time of gold mineralisation. **a** NE-SW section through the South Kalgurli shaft at 48,600 m grid north (modified from Stillwell 1929) showing the granodiorite porphyry emplaced into the D2a shear zone of the Lake View Lode (LVL). The dyke changes in dip at D2b faults on the upper levels. The D2a/D2b faults predate dyke intrusion but also record post-porphyry movement (D2c). The D3a Oroya Hanging Wall (OHW) Lode offsets granodiorite porphyry overprinted by sericite-ankerite alteration in the Paringa Basalt. The Paringa South shaft 7 level (see Fig. 9) is shown for reference. **b** Structural plan of the Judd and Perseverance shaft workings 335 m above sea level (modified from Stillwell 1929; Tomich 1952) showing two transverse diorite porphyry dykes, which crosscut a northwest striking granodiorite dyke but are displaced at D2a lodes and at D2b faults. D2a lodes: Australia Main (AML), Lake View (LVL), Tetley (TEL). Minerals: actinolite (act), albite (ab), ankerite (ank), calcite (cal), chlorite (chl), dolomite (dol), epidote (ep), muscovite (ms), paragonite (pg)

different times, although they were jointly mineralised during D2c or D3a reactivation.

Early (D3a) and late (D3b) reverse faults

In the Eastern Lode System, reverse faults oriented N40–60°W/35–50°SW are syn-mineralisation (D3a). They control the shallowly plunging, telluride-rich Oroya Shoot (Tomich 1959; Mueller et al. 1988). On the North Kalgurli shaft 15 to 18 levels, two reverse faults in Paringa Basalt displace D2a Fimiston Lodes but are locally ore grade (Finucane 1964). Published evidence for the D3a reactivation of older faults is limited to a single occurrence; ladder veins in the D2a GMF at Mt. Charlotte indicate a phase of syn-mineralisation oblique-

slip moving the Kalgoorlie Anticline up and northwest along a line pitching 60°SE (Mueller 2015).

In the Western Lode System, the reverse faults strike N20–40°W and are post-mineralisation (D3b). Most dip 20–55°SW, and a few conjugate ones dip northeast (Fig. 3). The sense of movement is almost pure dip-slip and varies from a few metres to 45 m (Feldtmann 1928; Tomich 1952; Wells 1964). A separate D3b structure is a weak but pervasive foliation defined by aligned alteration chlorite, sericite and carbonate. This foliation maintains a constant orientation of N40°W/80–90°SW throughout the deposit and overprints the sericite-ankerite-pyrite zones of Fimiston Lodes (Boulter et al. 1987). Auriferous pyrite-bearing veins striking at a high angle to the foliation are buckled as a result of low finite strain related to regional ENE-WSW shortening (Gauthier et al. 2007).

D4 dextral strike-slip faults

The district-scale Golden Pike Fault (GPF) varies in strike from north to N15°W (Fig. 1) and dips 65–70°SW. It offsets vertical Golden Mile Dolerite 2 km in a dextral sense, a geometry implying strike-slip. The D2a Golden Mile Fault is deformed and strikes parallel to the GPF in the northwest Golden Mile (Fig. 2). East dipping D2b faults close to the GMF record dextral strike-slip constrained by striations (0–25°N) and by the pitch-line intersection points of D2a Fimiston Lodes offset up to 70 m laterally. Drag structures indicate earlier east block up displacement (Finucane 1941), suggesting that these D2b faults were reactivated during movement on the D4 Golden Pike Fault.

The D4 Adelaide Fault at the southeast end of the Golden Mile strikes north-northwest, dips 75–80°SW and limits the extent of Fimiston Lodes to the northeast (Fig. 2). The fault displaces the greywacke syncline at the Lake View South shaft 150 m in a dextral sense, offsets the D2b Australia East Fault (Gauthier et al. 2004) and controls minor gold mineralisation at about 49,000 m grid north. The D4 Aberdare Fault (N17°W/80–90°W) is a parallel structure mined from three shafts (Fig. 2). Fault breccia within a zone of sericite-ankerite alteration contains auriferous arsenopyrite and pyrite but not telluride (Clout et al. 1990).

The Hannan Star Fault (N05°E/85°W) offsets the subvertical Kalgoorlie syncline 170 m in a dextral sense (Fig. 2), and is interpreted to displace the Adelaide Fault (Travis et al. 1971) suggesting a late or post-D4 timing. At Mt. Charlotte, faults of the same orientation link the west dipping Charlotte and Golden Pike faults (Fig. 1), and are thus part of the D4 system (Mueller 2015).

The D4 gold quartz-vein ore bodies at Mt. Charlotte are separated in time by barren D3b thrusts from the local D2a shear zones filled with telluride-bearing veins, indicating that Mt. Charlotte represents a younger hydrothermal system

(Mueller 2015). The D4 ore bodies are dated at 2655 ± 13 Ma (Rasmussen et al. 2009) and 2651 ± 9 Ma (Mueller et al. 2016; this issue) by xenotime Pb-Pb isochron and concordant U-Pb ages, respectively. Within the Golden Mile, D4 gold quartz-vein stockworks occur between and adjacent to branches of the Golden Pike Fault (Fig. 2). Veins of the Drysdale stockwork overprint the D2a Horseshoe No. 2 Lode (Clout et al. 1990), which is displaced by barren D3b reverse faults (Fig. 3).

Metamorphic and altered host rocks

The lodes of the Golden Mile occur within kilometre-scale, hydrothermal alteration zones extending from the Golden Mile in the southeast to Mt. Charlotte in the northwest (e.g. Travis et al. 1971; Mueller 2015). In the Paringa South mine, chlorite-calcite-ankerite alteration overprints the entire GMD, and sericite-ankerite alteration the upper Paringa Basalt. Although anomalous in gold (20–200 ppb) and part of the Golden Mile hydrothermal system, these zones are interpreted to predate pyrite-telluride mineralisation (Clout et al. 1990). A third alteration zone characterised by chloritoid, paragonite and ankerite is spatially associated with the D2a Trafalgar Fault southeast of the Golden Mile (Fig. 2). Whole-rock analyses of metamorphic and altered rocks are compiled in Appendix 2 of the Electronic Supplementary Material.
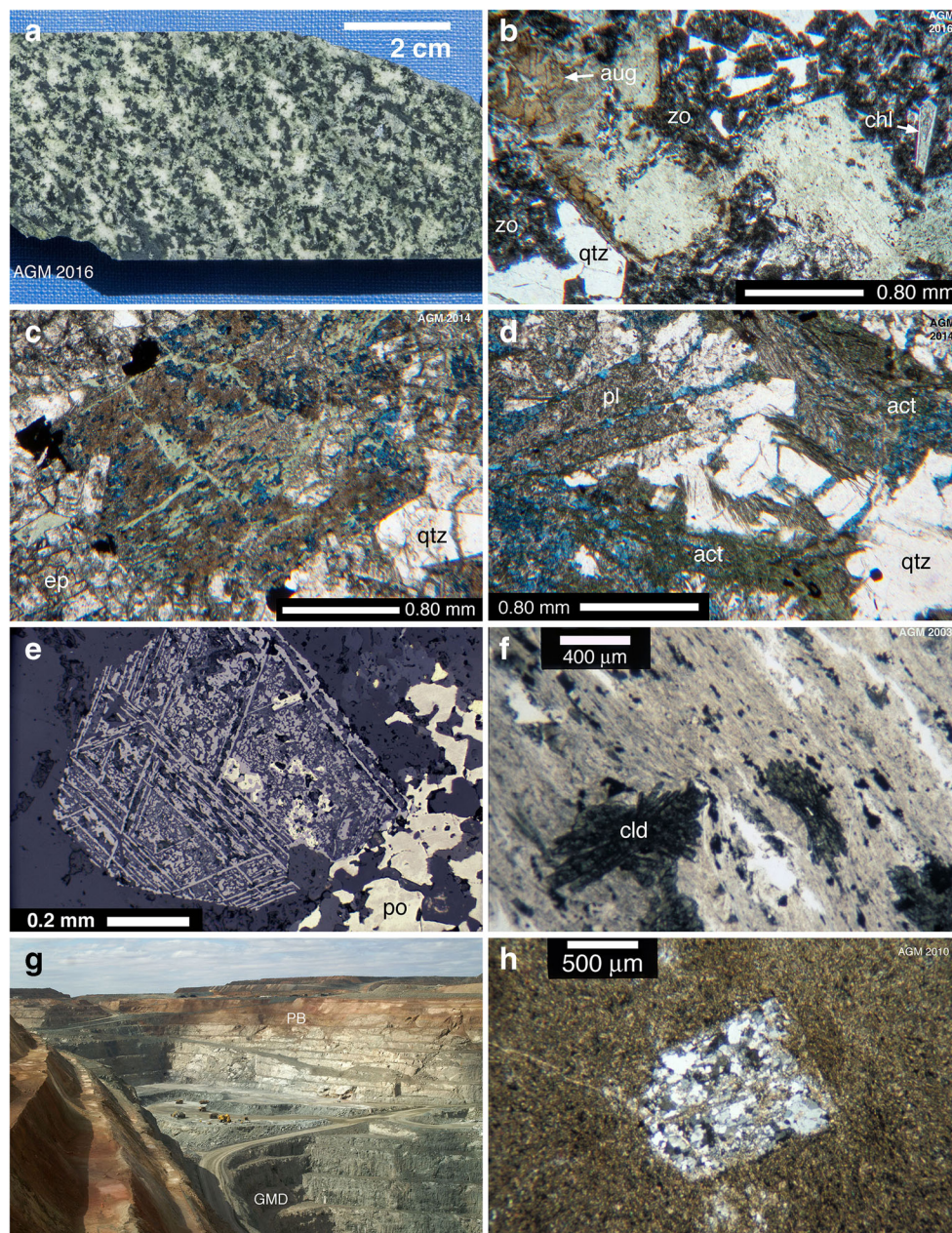
Metamorphic rocks

Greenschist facies metamorphic rocks underlie the surface laterite southwest (Fig. 2) and southeast of the Golden Mile. The pillow basalts consist of felted actinolite, and interstitial zoisite, epidote and albite (Thomson 1913; Stillwell 1929). In the Golden Mile Dolerite, the original igneous texture is preserved due to low D1 strain (Fig. 5a). Augite is pseudomorphed by uralite aggregates of tschermakite, acicular actinolite and accessory chlorite. Remnant augite is present locally (Fig. 5b). Calcic plagioclase is pseudomorphed by albite, microcrystalline granular zoisite and accessory epidote. Titanomagnetite is replaced by leuxoxene ± titanite enclosing embayed lamellae of igneous ilmenite. The actinolite-chlorite-albite-zoisite assemblage is assigned to the lower greenschist facies at estimated *P-T* conditions of 400–420 MPa and 320–390 °C (Mikucki and Roberts 2004; Goscombe and Blewett 2009).

Chlorite-calcite-ankerite alteration

Pervasive chlorite-calcite alteration associated with minor ankerite, sericite and magnetite extends 450 m into GMD southwest of the Golden Mile Fault (Fig. 3), and overprints the greenschist-facies actinolite-albite assemblage in the sill

Fig. 5 Greenschist-facies metamorphic (**a**, **b**) and hydrothermal mineral assemblages (**c–h**) in Golden Mile Dolerite (GMD) and in Paringa Basalt, Golden Mile deposit, Kalgoorlie. **a** Metamorphic GMD Unit 4: green uralite pseudomorphs of tschermakite-actinolite after augite, white albite-zoisite ± epidote pseudomorphs after calcic plagioclase, grey interstitial quartz (3 vol.%) and white leucoxene with ilmenite lamellae after Ti-magnetite (3–6 mm). Drill hole SE-13W1, 1527.0 m, the coin is 20 mm across. **b** Metamorphic GMD Unit 4: remnant igneous augite (aug) in pale green tschermakite-actinolite aggregates; calcic plagioclase is replaced by albite + zoisite (zo) ± epidote, and quartz (qtz) is interstitial. The pseudomorph of Fe-Mg chlorite (chl) may be after igneous hornblende. Drill hole SE-13W1, 1527.0 m, plane-polarised light. **c** Chlorite-calcite altered GMD Unit 4: rectangular pseudomorph of green chlorite, calcite (*stained pink*) and Fe-calcite (*stained blue*) after igneous augite, sericitised albite laths, interstitial quartz (qtz), chlorite and epidote (ep), Perseverance shaft 23 level, UWA no. 51646, plane-polarised light. **d** Chlorite-ankerite altered GMD Unit 8: green chlorite, dolomite, ankerite (*stained blue*) and trace sericite replace plagioclase (pl) and

metamorphic actinolite (act) in pseudomorphs preserving the igneous texture in matrix quartz (qtz), Golden Pike shaft 5 level, UWA no. 51672, plane-polarised light. **e** Chlorite-ankerite altered GMD Unit 8: rutile outlines former Ti-magnetite in a matrix of chlorite, ankerite and pyrrhotite (po), Mt. Charlotte mine 22 level, UWA no. 109744, plane-polarised reflected light. **f** Chloritoid-paragonite-ankerite altered GMD Unit 9: rosettes of post-kinematic chloritoid (cld) in paragonite-ankerite-quartz schist of the D2a Trafalgar Fault. Drill hole TRF-2, 145.7 m, plane-polarised light. **g** Sericite-ankerite altered Paringa Basalt: looking N30°E at green-grey chloritic Golden Mile Dolerite (GMD) of the Brownhill Syncline. Light brown sericite-ankerite altered Paringa Basalt (PB) forms the distant high wall. Visitor platform (UTM 6593943 m N, 356338 m E, +385 m), October 2006, bench heights are 10–30 m. **h** Sericite-ankerite altered Paringa Basalt: plagioclase phenocryst replaced by mosaic-textured albite (metamorphic?). The albite mosaic is partly replaced by the sericite-ankerite-quartz matrix. Paringa South shaft 4 level, UWA no. 102397, crossed polars

northeast of the fault leaving small remnants of metamorphic rock (Stillwell 1929; Bartram and McCall 1971). Further northeast, the chlorite-calcite zone extends in Paringa Basalt across the D1 Kalgoorlie Anticline into the Eureka facies of the GMD sill.

In Golden Mile Dolerite, chlorite and Fe-calcite selectively replace metamorphic amphibole in the pyroxene sites, and albite ± calcite ± sericite replace all zoisite in plagioclase sites still preserving the igneous texture (Fig. 5c). Carbon dioxide, water and K_2O are enriched relative to local meta-gabbro (App. 2). In parts of the zone, alteration epidote is present (Fig. 5c), suggesting an affinity to propylitic alteration in the sense of Meyer and Hemley (1967).

In the competent iron-rich units of the GMD sill, in particular the granophyric GMD Unit 8 (Fig. 3), chlorite and ankerite replace the pyroxene sites and parts of the plagioclase sites (Fig. 5d) in association with minor (5–10%) sericite or siderite and magnetite (Phillips 1986; Clout et al. 1990). Rutile pseudomorphs after Ti-magnetite (Fig. 5e) permit the distinction of petrographic units within the sill. Selective replacement preserving texture grades locally into jig-saw breccia of higher magnetite ± hematite content cemented by ankerite, siderite and chlorite. The chlorite-ankerite zones are tens of metres wide and do not display a spatial relationship to the pyrite-telluride lodes (Gauthier 2006).

Chloritoid-paragonite-ankerite alteration

Diamond holes drilled at the southeast margin of the Golden Mile deposit outlined a zone of chloritoid-bearing alteration in GMD more than 240 m wide and 1000 m long (Prider 1947). Re-logging of the drill core revealed a wide zone (>80 m) of paragonite-ankerite-quartz-albite schist (50–100 ppb Au) centred on the D2a Trafalgar Fault. The schist is characterised by chloritoid aggregates (5–20 vol.%; Fig. 5f) and by spaced bands of disseminated pyrite. It is bordered by weakly strained GMD Unit 9, which contains less chloritoid (1–5%) and albite. Pyroxene sites are pseudomorphed by ankerite-chlorite ± magnetite, and plagioclase sites by paragonite and quartz. The petrography of the zone is described in Part 2 of the Paringa South study (this issue).

Two other localities at the southeast margin of the Golden Mile suggest that chloritoid-bearing alteration extends far beyond the Trafalgar Fault. The first is at the former Lake View town site (LVT in Fig. 2). Samples collected from shafts sunk in GMD Unit 9 all contain chloritoid (5–15 vol.%), and consist of chlorite-quartz-ankerite-magnetite rock (App. 2), chlorite schist and breccia, magnetite- and pyrite-bearing paragonite-chlorite-quartz-ankerite schist and tourmaline-bearing paragonite-quartz schist (Simpson 1930). The second locality is southeast of the Chaffers shaft (Fig. 2) on the −90 m level of the former Hannan's Star mine, where chloritoid forms pseudomorphs after pyroxene in sericite-ankerite

altered Golden Mile Dolerite close to the contact of a porphyry dyke (Thomson 1913).

Sericite-ankerite alteration

The chloritoid-paragonite-ankerite zone of the Trafalgar Fault merges with the 150-m-wide sericite-ankerite zone, which rims the Kalgoorlie Anticline and "bleaches" the upper Paringa Basalt along its contact with Golden Mile Dolerite (Figs. 2 and 3). Bleached Paringa Basalt is exposed in the Paringa South (Fig. 5g), North Kalgurli and South Kalgurli mines on all levels down to 585 m below surface (Feldtmann 1928; Finucane 1964). XRD analyses show that the altered basalt consists of fine-grained ankerite, quartz and muscovite, minor albite and paragonite (interlayered with muscovite) and accessory rutile. Carbon dioxide and potassium are strongly enriched (App. 2). Pillow structures are preserved, and plagioclase phenocrysts are unstrained but replaced by granular albite (Fig. 5h). The phenocryst sites are embayed and crossed by sericite-quartz-ankerite veinlets, indicating that the alteration is feldspar destructive, and that part of the albite is probably of metamorphic origin. Chlorite and magnetite porphyroblasts occur locally (Thomson 1913).

The Paringa Basalt contact zone dips southwest and joins the sub-vertical Golden Mile Fault at depth (Fig. 3). Like the contact zone, the carbonaceous schist and greywacke of the GMF and all porphyry dykes within are pervasively altered to a sericite-carbonate assemblage. Whole-rock analyses (App. 2) and limited petrographic data suggest that the alteration assemblage comprises muscovite, ferroan dolomite and minor ankerite, Fe-Mg chlorite and albite (Stillwell 1929; Mueller 2015).

Porphyry dykes and time constraints

Calc-alkaline hornblende-plagioclase porphyry dykes 0.5 to 30 m thick and up to hundreds of metres long are emplaced into carbonaceous schist of the D2a Golden Mile Fault (Fig. 6a), and into adjacent D2a shear zones like the Lake View Lode (Fig. 4a). Southeast of the Golden Mile, drill hole SE-1 intersected a porphyry complex 280 m thick, perhaps composed of two dykes, which is located between the GMF and the Lake View Lode (Fig. 1). All dykes are altered, and are massive to moderately strained. In the GMF and at dyke contacts, especially those followed by Fimiston Lodes, the dykes are overprinted by feldspar-destructive muscovite-dolomite alteration (Fig. 6b). Plagioclase phenocrysts are embayed; hornblende phenocrysts are pseudomorphed by Fe-dolomite, rutile and Cr-muscovite (0.3–0.6 wt.% Cr_2O_3; Stillwell 1929); and quartz phenocrysts are preserved. Quartz, albite and dolomite fill veins. Tourmaline and pyrite are disseminated. Away from contacts and in chloritic GMD, the dykes are
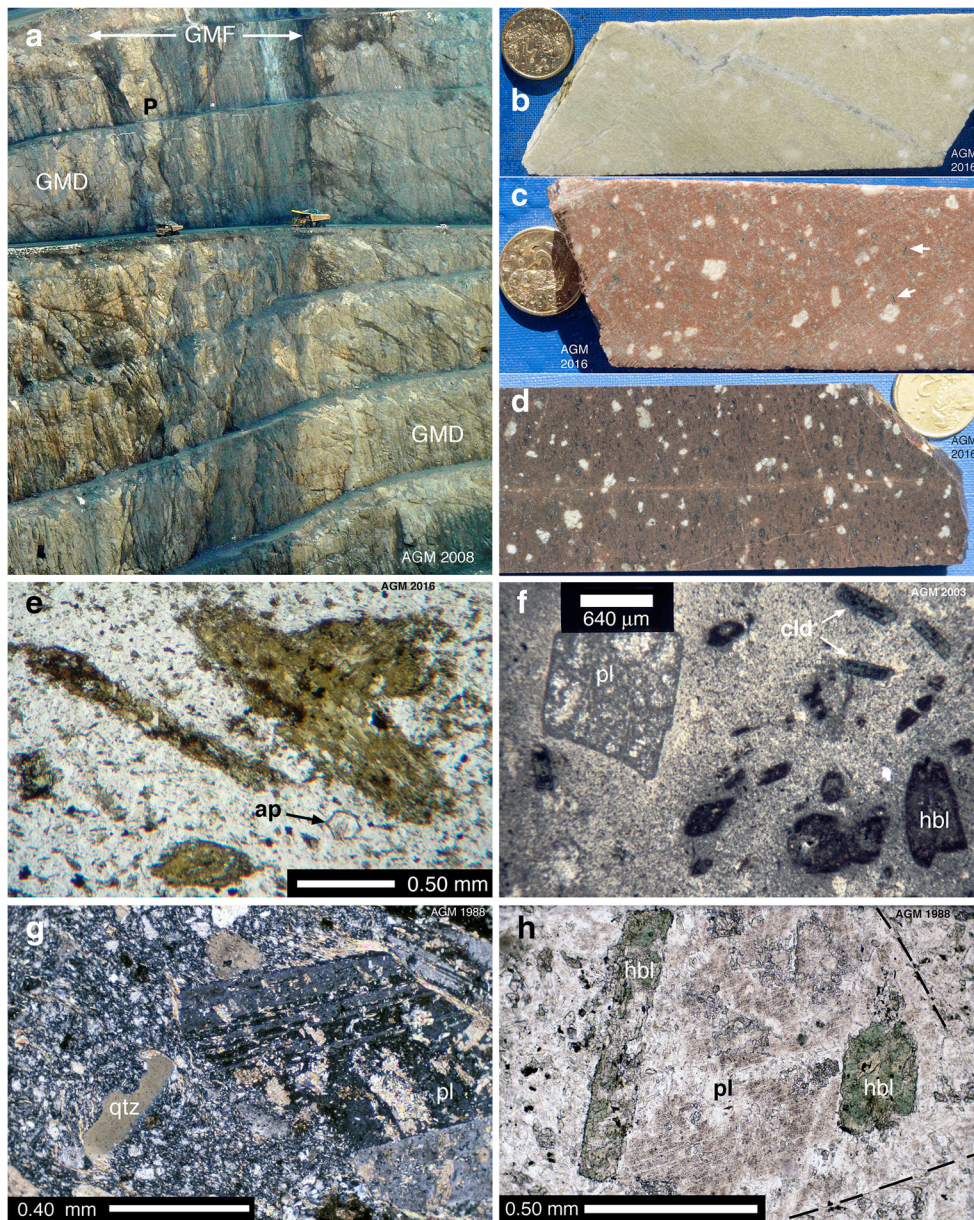
Fig. 6 Igneous and hydrothermal minerals in granodiorite and diorite porphyry, Golden Mile deposit, Kalgoorlie. **a** D2a Golden Mile Fault (GMF): looking S50°E at black carbonaceous schist and foliation-parallel porphyry dykes (P) altered to sericite and Fe-dolomite. The GMF and the adjacent chlorite-calcite altered Golden Mile Dolerite (GMD) are displaced by shallowly dipping, barren D3b reverse faults. Visitor platform, July 2008, bench heights are 10–30 m. **b** Southeast porphyry complex: granodiorite overprinted by sericite-quartz-dolomite ± pyrite alteration, embayed plagioclase phenocrysts (*white*), sericite-rutile pseudomorphs after hornblende, quartz-dolomite veins. Drill hole SE-1, 212.4 m, the coin is 20 mm across. **c** Southeast porphyry complex: granodiorite overprinted by hematite-bearing sericite-chlorite-dolomite alteration, white subhedral plagioclase phenocrysts, green chlorite-dolomite-rutile pseudomorphs after hornblende (*arrows*), 1 vol.% pyrite. Drill hole SE-1, 215.6 m, the coin is 20 mm. **d** Southeast porphyry complex: granodiorite overprinted by early biotite alteration, white subhedral plagioclase phenocrysts and glomerocrysts, brown biotite pseudomorphs after hornblende phenocrysts, the groundmass contains plagioclase microlites and 5 vol.% disseminated biotite,

crosscutting quartz-albite-dolomite-chlorite veinlet. Drill hole SE-1, 292.7 m, the coin is 20 mm. **e** Southeast porphyry complex: granodiorite, hornblende phenocrysts and glomerocrysts are selectively replaced by biotite ± rutile, the seriate-textured plagioclase groundmass contains apatite (ap) and biotite. Drill hole SE-1, 292.7 m, plane-polarised light. **f** D2a Trafalgar Fault: granodiorite (?) porphyry, chloritoid porphyroblasts (cld), ankerite-rutile pseudomorphs after hornblende (hbl) and a plagioclase phenocryst (pl) partly replaced by ankerite and sericite. Much of the groundmass is altered to paragonite-ankerite ± tourmaline. Drill hole TRF-5, 134.1 m, plane-polarised light. **g** D2a Lake View Lode: granodiorite porphyry, twinned plagioclase glomerocryst (pl) and embayed quartz phenocryst (qtz) in granular quartz-albite groundmass. Sericite-dolomite alteration, sericite pressure shadows at phenocrysts. Perseverance shaft 3 level, UWA no. 97474, crossed polars. **h** Diorite porphyry: a plagioclase phenocryst (pl, *dashed line*) encloses and is in contact with hornblende (hbl) replaced by Mg-chlorite. Part of the plagioclase is altered to dolomite and sericite. South Kalgurli shaft −305 m level, 80 m northwest of the Morty shaft, UWA no. 59057, plane-polarised light

altered to a chlorite-muscovite-dolomite assemblage coloured red by disseminated hematite and pyrite. Plagioclase phenocrysts are well preserved (Fig. 6c), and hornblende phenocrysts are pseudomorphed by Mg-Fe chlorite, Fe-dolomite and rutile. Early barren biotite alteration, characterised by the selective replacement of hornblende by biotite ± rutile (Fig. 6d, e), is absent within the Golden Mile and restricted to the central part of the porphyry complex intersected by drill hole SE-1. Dykes emplaced into the D2a Trafalgar Fault are overprinted by chloritoid-paragonite-ankerite alteration (Fig. 6f).

Pre-mineralisation granodiorite dykes

The main suite of altered dykes, termed "albite porphyries" in Stillwell (1929), is characterised by embayed to subhedral quartz, plagioclase and hornblende phenocrysts. In the total silica (anhydrous) versus Zr/TiO_2 and Nb/Y diagrams of Winchester and Floyd (1977), these dykes plot in the calc-alkaline dacite/rhyodacite field (Table 1), and are thus classified as granodiorite. They are abundant in the GMF and common in D2a shear zones of the Eastern Lode System (Stillwell 1929). Most strike northwest, dip steeply (Fig. 3) and show no evidence of post-emplacement folding or rotation (e.g. Gauthier et al. 2007). The most precise U-Pb age for this suite, dated at three localities within the Kalgoorlie district, is 2674 ± 6 Ma (Kent and McDougall 1995).

In contrast to phenocrysts in the Paringa Basalt (Fig. 5h), neither the quartz, nor the twinned plagioclase phenocrysts and glomerocrysts (Fig. 6g), nor plagioclase microlites in the groundmass are recrystallised to a granular mosaic, suggesting that these dykes post-date the peak of greenschist-facies D1 metamorphism. The granodiorite dykes are overprinted by wall-rock alteration in the D2a Golden Mile Fault (Fig. 6a), in the Paringa Basalt contact zone (Fig. 4a) and in the D2a Trafalgar Fault (Fig. 6f), indicating that the kilometre-scale alteration zones described above are younger than 2674 ± 6 Ma.

Syn-mineralisation diorite and kersantite dykes

Dykes of a second suite are termed "chloritised hornblende porphyries" in Stillwell (1929) due to their abundance of hornblende pseudomorphs (Fig. 6h) and scarcity of plagioclase and quartz phenocrysts. Lath-shaped plagioclase microlites are common imparting a trachytic or seriate texture to the groundmass (Stillwell 1929). The hornblende porphyries plot in the andesite (diorite) field of the Winchester and Floyd (1977) diagrams, and display high chromium (96–211 ppm), nickel (64–107 ppm) and vanadium contents (Table 1), a geochemical signature shared with intrusions of the high-Mg monzodiorite-

granodiorite-tonalite suite (2662 ± 6 to 2658 ± 3 Ma) emplaced 12 km southeast of the Golden Mile into the D2a Boulder Lefroy-Golden Mile fault system (Mueller 2007).

Although most diorite porphyries are sub-parallel to granodiorite dykes, as both are emplaced into northwest striking D2a shear zones, they are the only dykes oriented in a transverse northeast strike direction (Stillwell 1929). The transverse dykes dip 70–80°NW or SE, crosscut older granodiorite dykes and are offset by syn-mineralisation D2c movement at D2a shear zones and D2b faults (Fig. 4b). The transverse diorite dyke (N40°E/80°SE) southeast of the Judd shaft is traced with little apparent offset over a strike length of 400 m up to the Golden Mile Fault, and persists from +335 m above down to the sea level (Stillwell 1929). Gauthier et al. (2007) report that the diorite porphyries crosscut auriferous veins, contain xenoliths of magnetite-carbonate and pyrite-tourmaline ore and are therefore synchronous with mineralisation. One dyke (N45°W/54°SW) on the Chaffers shaft 20 level is dated at 2663 ± 11 Ma by an intercept U-Pb age (Gauthier et al. 2007).

Another possible syn-mineralisation dyke is the chlorite-dolomite altered kersantite on the Paringa South shaft 6 level, hosted by sericite-ankerite altered Paringa Basalt and oriented N65°E/85°NW parallel to extension veins in the D3a Oroya shear system (Mueller et al. 1988). The dyke is characterised by chloritised biotite and by apatite phenocrysts, and is enriched in arsenic and silver (Table 1). SHRIMP zircon U-Pb analyses define a reversely discordant $^{207}Pb/^{206}Pb$ age of 2642 ± 6 Ma (McNaughton et al. 2005). The reverse discordance is attributed to matrix effects caused by high trace element contents relative to the pure zircon standard. In contrast, the TIMS analyses of nine zircon fragments are normally discordant in the U-Pb system (Urs Schaltegger, personal communications 2003). Given the lead loss, the Pb-Pb age of 2642 ± 6 Ma is interpreted as a minimum for kersantite emplacement.

The Fimiston lode system

Gustafson and Miller (1937) recognised that the lodes form identical geometric arrays on both sides of the Kalgoorlie Syncline, and divided the ore bodies according to strike direction into Main, Caunter and Cross Lodes. High-grade shoots occur at lode intersections, and plunge 50–60°SE (Tomich 1952; Finucane and Jensen 1953; Wells 1964; Mueller et al. 1988).

Main Lodes

The Main Lodes include D2a shear zones of two different orientations. The first group is parallel in strike and dip to

Table 1 Whole-rock major oxide and trace element analyses of least-altered calc-alkaline porphyry and lamprophyre dykes, Golden Mile and Mt. Charlotte, Kalgoorlie, Western Australia

Mine/drill hole	North Kalgurli	Boulder Main	Perseverance	South End SE-1	Sth Kalgurli	Mt. Charlotte	Paringa Sth
Level/depth	800 ft	2,050 ft	3 level (LVL)	290–294 m	1,000 ft	22 level	6 level
UWA no.	59259	59258	97474	59224	59057	109751	109708
Strike/dip	Not known	NNW/±90°	NW/80°NE	NNW/±90°	NNW/85°W	N20°E/75°E	N65°E/85°NW
Classification	Dacite	Rhyodacite	Dacite	Dacite	Andesite	Andesite	Kersantite
Phenocrysts	pl, hbl	pl, qtz, hbl	pl, qtz, hbl	hbl, pl	hbl, pl	hbl	bt, ap
Alteration	ms-cb ± ab	ms-cb	ms-cb ± ab	bt, late chl-cb	chl-cb ± ms	chl-dol-ab	chl-dol-qtz
SiO_2 (wt.%)	62.61	68.99	61.90	66.07	57.24	57.20	30.39
TiO_2	0.62	0.45	0.45	0.55	0.76	0.68	2.21
Al_2O_3	14.93	16.07	13.87	15.81	15.30	13.35	7.01
Fe_2O_3	1.69	0.21	0.50	2.07	1.35	0.46	0.54
FeO	2.18	1.90	2.80	1.46	3.39	4.33	7.25
MnO	0.05	0.02	0.05	0.06	0.07	0.08	0.12
MgO	3.67	1.38	1.78	3.03	3.83	3.75	11.47
CaO	3.12	2.07	3.96	1.38	4.00	4.95	17.01
Na_2O	5.17	2.92	5.18	6.42	4.52	2.91	<0.02
K_2O	2.13	3.16	1.53	1.17	1.87	2.12	0.02
P_2O_5	0.18	0.12	0.16	0.17	0.43	0.18	5.36
L.O.I.	3.75	3.80	6.78	1.59	7.51	8.83	17.28
Total	100.10	101.09	98.96	99.78	100.27	98.84	98.66
CO_2 (wt.%)	3.60	2.42	4.82	0.86	6.48	6.30	13.37
Density (g/cm^3)	2.73	2.74	2.72	n.a.	2.74	2.76	2.92
Sulphur (ppm)	468	7,230	200	156	257	500	450
Ag (ppm)	<0.1	0.1	<0.1	<0.1	0.1	0.1	0.3
As	14	37	9	6	16	13	215
Ba	651	1,700	887	771	547	510	191
Be	1.3	1.9	1.4	1.0	1.0	1.4	0.9
Co	<3	3	9	10	16	17	23
Cr	52	27	45	30	96	211	206
Cs	22	14	5.5	4.2	8.8	3.1	2.5
Cu	15	8	29	9	39	<2	16
Ga	21	25	21	21	18	20	14
Hf	3.6	3.4	3.4	3.2	3.3	3.4	19
Li	9.1	13	11	24	45	18	101
Mo	0.2	0.3	0.1	0.2	1.2	<0.1	<0.1
Nb	4	2	5	2	3	4	23
Ni	19	10	24	32	64	107	297
Pb	4	18	6	14	6	5	40
Rb	61	81	46	39	43	54	4
Sb	4.9	4.9	5.8	0.4	2.7	1.8	7.3
Sc	10	7	n.a.	5	16	10	21
Sn	0.9	1.2	0.7	1.2	1.0	0.7	2.5
Sr	256	413	404	438	375	199	2,722
Ta	0.18	0.21	0.17	0.12	0.39	0.19	2.1
Th	4.7	5.3	4.5	5.1	6.0	4.5	26
Tl	0.50	0.88	0.40	0.33	0.36	0.45	<0.5
U	1.2	1.3	1.0	1.6	1.2	0.98	3.0
V	82	48	52	51	120	91	117
W	4.3	7.3	7.6	0.4	5.7	4.2	1.2
Y	10	4	8	7	12	13	65

Table 1 (continued)

Mine/drill hole	North Kalgurli	Boulder Main	Perseverance	South End SE-1	Sth Kalgurli	Mt. Charlotte	Paringa Sth
Level/depth	800 ft	2,050 ft	3 level (LVL)	290–294 m	1,000 ft	22 level	6 level
UWA no.	59259	59258	97474	59224	59057	109751	109708
Strike/dip	Not known	NNW/±90°	NW/80°NE	NNW/±90°	NNW/85°W	N20°E/75°E	N65°E/85°NW
Classification	Dacite	Rhyodacite	Dacite	Dacite	Andesite	Andesite	Kersantite
Phenocrysts	pl, hbl	pl, qtz, hbl	pl, qtz, hbl	hbl, pl	hbl, pl	hbl	bt, ap
Alteration	ms-cb ± ab	ms-cb	ms-cb ± ab	bt, late chl-cb	chl-cb ± ms	chl-dol-ab	chl-dol-qtz
Zn (ppm)	40	28	61	105	102	74	165
Zr (ICP-MS)	132	132	130	125	127	144	738
Zr (XRF)	139	136	138	n.a.	137	140	744
La	29	27	26	n.a.	51	25	475
Ce	59	55	53	n.a.	117	53	1,188
Pr	6.8	6.3	6.2	n.a.	15	6.2	150
Nd	27	24	24	n.a.	59	25	563
Sm	4.5	3.9	4.2	n.a.	9.3	4.5	85
Eu	1.2	1.1	1.1	n.a.	2.4	1.2	19
Gd	3.1	2.3	2.9	n.a.	5.5	3.3	39
Tb	0.41	0.26	0.38	n.a.	0.65	0.41	3.5
Dy	2.0	1.2	1.9	n.a.	2.8	2.3	18
Er	0.85	0.43	0.84	n.a.	1.0	0.97	5.0
Yb	0.78	0.36	0.74	n.a.	0.88	0.99	2.4
Lu	0.11	0.05	0.10	n.a.	0.13	0.13	0.70
Classification after Winchester and Floyd (1977)							
SiO_2 (anhydrous)	65.05	71.68	66.45	67.14	61.87	62.81	36.84
Zr/TiO_2	0.022	0.030	0.031	0.023	0.018	0.021	0.034
Nb/Y	0.400	0.500	0.625	0.286	0.250	0.308	0.354

UWA no. = E. de C. Clarke Earth Science Museum, the University of Western Australia. Major oxides of UWA nos. 59,057 to 59,259 partly from O'Beirne (1968). SE-1 trace element data from Nixon (2015). Samples pulverised in an agate mill. Major oxides by X-ray fluorescence (XRF) fused glass disc (Norrish and Hutton 1969). Loss on ignition (L.O.I.) at 1000 °C. Carbon dioxide by Leco furnace (Lee 1980). Sulphur and phosphorus by inductively coupled plasma optical emission spectroscopy (ICP-OES). FeO by titration. Elements by XRF pressed powder pellet: Ba, Co, Cr, Cu, Ga, Nb, Ni, Pb, Rb, Sc, Sr, V, Y, Zn, Zr. Other trace elements by inductively coupled plasma mass spectrometry (ICP-MS) after hydrofluoric or mixed acid digest. XRF analyses at the University of Western Australia, ICP analyses at Intertek-Genalysis, Perth. Detection limits: major oxides and carbon dioxide 0.01–0.05 wt.%, sulphur 20 ppm, phosphorus 10 ppm. Trace elements by XRF 1–5 ppm, trace elements by ICP-MS 0.01–0.1 ppm. Below detection (ppm): Bi (<0.1), Re (<0.01), Te (<0.1)

LVL Lake View Lode, *n.a.* not analysed, *ab* albite, *ap* apatite, *bt* biotite, *cb* carbonate, *chl* chlorite, *dol* dolomite, *hbl* hornblende, *ms* muscovite, *pl* plagioclase, *qtz* quartz

the segment of the Golden Mile Fault (N40–45°W/80°SW) not deformed by drag on the D4 Golden Pike Fault, and is represented by the Lake View Lode in the Eastern System (Figs. 2 and 3). The average orientation of Group 1 Main Lodes on the Perseverance shaft 3, 9 and 15 levels is N40°W/85°SW (Ion 1982).

The second group of Main Lodes strikes N30°W, dips vertically and is represented by the Horseshoe No. 3 and No. 4 Lodes in the Western System (Figs. 2 and 3). Both lodes intersect the Golden Mile fault zone, and displace the lithologic contact GMD Unit 10-Black Flag greywacke 100–180 m southwest block south (Finucane and Jensen 1953). The structural setting of the No. 4 Lode (≥200 t Au pre-1973 production; Keats 1987) is illustrated in plan, cross and longitudinal section (Fig. 7). The

greywacke wedge faulted by the lode plunges 60°SE, and high-grade ore persists down-plunge to the 3140 ft (−957 m) level of the Golden Horseshoe mine (Stillwell 1929). The vertical No. 4 Lode cuts across a foliation (D1?) in altered Golden Mile Dolerite dipping 65–75°SW, and slickenside planes parallel to the lode are marked by horizontal striations (Larcombe 1913). The No. 3 Lode offsets the southwest dipping No. 2 Lode, and forms the boundary of the Morrison Lode (Figs. 2 and 3).

Caunter and Cross Lodes

Most Caunter Lodes are D2a shear zones branching off and terminating at Main Lodes (Gustafson and Miller 1937). They

are abundant in both the Western and Eastern Lode Systems. Their average orientation on the Perseverance shaft 3, 9 and 15 levels is N55–60°W/65–70°SW (Ion 1982).

Other Caunter Lodes strike N70–90°W, dip 55–70°SSW and consist of a hanging wall fault-fill vein connected to spur veins striking 25–40° clockwise into the footwall. A few are composed of sigmoidal veins arranged en echelon within a zone striking N80°W (Finucane 1948). Porphyry dykes are offset up to 30 m north block east in plan section indicating a dextral component of movement (Fig. 4b). In contrast, Gauthier et al. (2004) mapped a sinistral drag fold in the diorite porphyry dyke displaced by the Morrison Lode (N80°W) at the south end of the Western System (Fig. 7a). Wells (1964) interprets such Caunter Lodes as normal faults.

Cross Lodes strike N40°E and dip steeply northwest or southeast (Gustafson and Miller 1937). In the Perseverance mine, they have an average orientation of N35–40°E/80°SE but are less abundant than the Main and Caunter Lodes. They consist of a pyrite-rich siliceous core, locally brecciated, and sericite-ankerite replacement up to 3 m wide (Ion 1982). The Phantom Lodes represent a group of D2a Caunter and Cross Lodes linking Main Lode ore bodies at the contact of a diorite porphyry dyke with the principal surface of the Golden Mile Fault (Fig. 7a, b). One Caunter and one Cross Lode of this group crosscut a D2b fault of the Australia East system but differ in grade across this fault (Finucane 1941, 1948; Baker 1958), structural relations consistent with the post-D2b timing of mineralisation outlined above.

Structural setting, Paringa South mine

The lease of the Paringa South mine covers the Brownhill Syncline, the subsidiary D1 fold on the southwest limb of the Kalgoorlie Anticline (Fig. 2). The lodes and faults displacing the syncline are shown on three level plans, on a cross section through the Paringa South shaft and on a longitudinal projection through the hinge of the syncline. Grid north strikes N38°W parallel to the Main Lode direction. The classification of all structures is according to the relative time of formation (D1, D2a, D2b, D3a). The D2a and D2b faults predate mineralisation, which is synchronous with D2c strike-slip reactivation and D3a reverse faulting. The D2a faults traced by Fimiston Lodes are interpreted as part of the Riedel system defined in the terminology section.

D1 Brownhill Syncline

The Brownhill Syncline is outlined by the contact between chlorite-ankerite altered GMD and sericite-ankerite altered Paringa Basalt. Lenses of thin-bedded carbonaceous greywacke, pervasively altered to sericite and ferroan dolomite, line the contact of the discordant GMD sill. On level

6 at 49,310 m north in the OHW Lode drive, a 1–2 m thick bed of clast-supported pillow breccia overlies coherent pillow basalt below greywacke. On level 11, bleached pillow basalt is exposed 50 m below the hinge of the syncline. The pillows, commonly 25 × 45 cm in cross section and 75 cm long, are flattened but not stretched in the plane of foliation. This foliation, perhaps axial planar to the D1 folds, has an average orientation of N40°W/70–80°SW in chloritic GMD on levels of the North Kalgurli and Paringa South mines. Third-order folds such as the Paringa Anticline occur on both limbs of the syncline, which maintains a shallow southeast plunge towards the Iron Duke shaft (Fig. 8). On level 7, the Paringa Anticline is uplifted at the D2b A-Lode Fault, and the plunge of the syncline reverses at the Pomeroy shaft (Fig. 9).

### D2a Main Lodes (principal displacement zones)

The B-Lode extends over a strike of 2 km from the Paringa South shaft to the Golden Pike Fault (Fig. 1). Close to the shaft, the lode crosses from the Golden Mile Dolerite into Paringa Basalt, offsets the contact about 100 m in a sinistral sense and branches into the footwall Main Lode (N40°W/70°SW) and the hanging wall West Lode, both connected by subsidiary Riedel shear zones (N50–60°W/50–70°SW; Fig. 8). The two boundary lodes merge down dip (Fig. 10). Stopes are 1–3 m wide.

The Kelly Lode on the Paringa South 4 level, oriented N40°W/60–70°SW, develops at 49,180 m N in chlorite-calcite altered Golden Mile Dolerite as a single brecciated fault-fill vein, widens into a network of veins with muscovite-ankerite-pyrite selvages at 49,270 m N and broadens into a pervasive ore-grade replacement zone at 49,305 m N (Fig. 11a–c). The lode offsets the contact GMD Unit 1/2 about 15 m in a sinistral sense (Fig. 8). Striations defined by pyrite aggregates on slickenside planes of the footwall vein pitch 10–20°SE indicating strike-slip with a small normal component southwest block down.

The Lake View Lode is the principal mineralised structure in the North Kalgurli mine (Fig. 9). In Golden Mile Dolerite, it forms a series of southwest stepping branch lodes, which vary in strike from N40°W to N50°W and dip 60–75°SW. Most stopes are 1–3 m wide.

D2a Main Lodes (P shear zones)

The Federal Lode strikes N25–30°W, dips 75–90°SW and forms an acute angle of 10–15° in strike to the Golden Mile Fault, like the Horseshoe No. 4 Lode in the Western System. The lode offsets the GMD-Paringa Basalt contact 65 m in a sinistral sense (Fig. 8). On level 6 in the 605 stope, the Federal Lode is 3 m thick, strikes N35°W/90° and contains extensional ladder veins oriented N52°E/70°NW. The veins imply movement along a line pitching 20°SE on the lode walls.
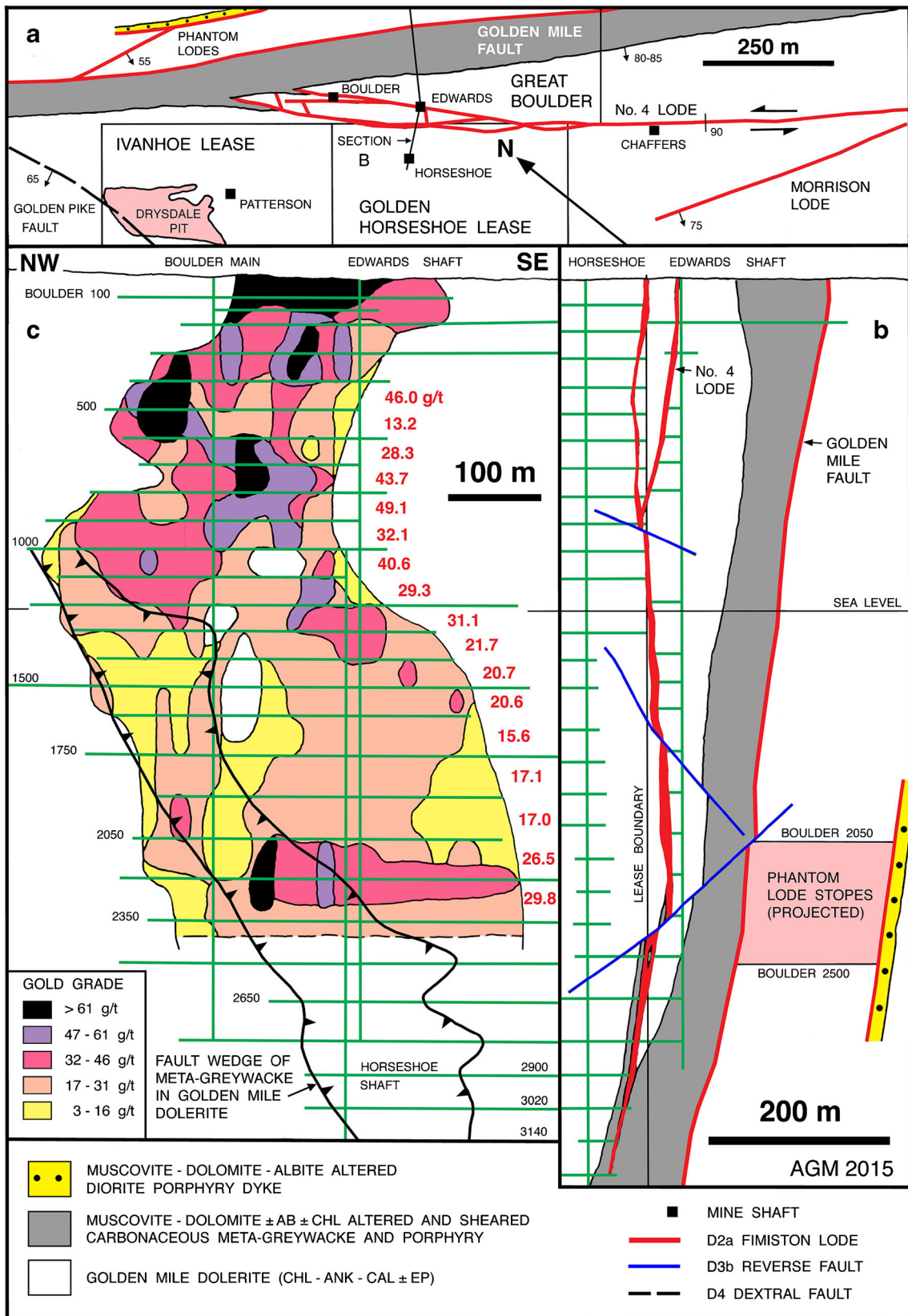
◀ **Fig. 7** Structural setting of the D2a Horseshoe No. 4 Lode, Western Lode System, Golden Mile, Kalgoorlie. The structures are ordered according to the time of formation (D2a to D4), and not according to the time of gold mineralisation. The D3b reverse faults are barren. **a** Structural plan at 350 m above sea level modified from a 1984 open pit map provided by Kalgoorlie Mining Associates. The Drysdale pit was centred on the D2a Horseshoe No. 2 Lode and on D4 gold quartz veins in GMD Unit 8. The position of the Phantom Caunter Lodes (projected) is approximate. **b** Cross section through the Golden Horseshoe and Edwards shafts (modified from Stillwell 1929) showing the intersection of the No. 4 Lode with the greywacke-porphyry complex of the D2a Golden Mile Fault. The Phantom Caunter Lodes (projected) link the Golden Mile Fault and Main Lode ore bodies at the contact of the diorite dyke (Baker 1958). **c** Longitudinal projection of gold grade in the No. 4 Lode close to the intersection with the GMD Unit 10-greywacke lithologic contact (modified from Larcombe 1913). The grade above the 1000 ft (−305 m) level represents the east branch of the lode, and the grade below the main west branch. The southeast limit of gold grade is defined by the Great Boulder-Golden Horseshoe lease boundary. The outline of the faulted lithologic contact is from Stillwell (1929), and the average gold grade of each block between levels from Beyschlag et al. (1916)

The Federal Lode is associated with narrow hanging wall lodes of similar strike and dip (Fig. 10). In sericite-ankerite altered Paringa Basalt, the lodes of the Federal system are narrow (10–50 cm) and composed of pinch-and-swell veins, foliated breccia and S-C mylonite (e.g. Fig. 11d).

D2a Caunter Lodes (R and T shear zones)

The B-Lode initiates southeast of the Paringa South shaft in a broad array of Riedel shear zones (N55–60°W/65–80°SW) terminating at the Lake View Lode, a structural setting displayed on the 7 level plan (Fig. 9). A prominent set of Caunter Lodes branches off the B-Lode at about 48,900 m grid north on the Paringa South 4 level (Fig. 8). These lodes consist of muscovite-ankerite-pyrite replacement up to 1 m thick, strike N60–70°W and vary in dip from 70° (No. 1 Caunter) to 40°SW, the moderate dip suggesting a component of normal movement. If sorted by strike relative to the bounding Main Lode, the Caunter Lodes fall into two groups: one with anticlockwise strike angles of 15–30° ($n = 12$) and another with anticlockwise strike angles of 36–48° ($n = 10$). A few lodes strike N75–85°E, dip 65–80°SSE or NNW and are
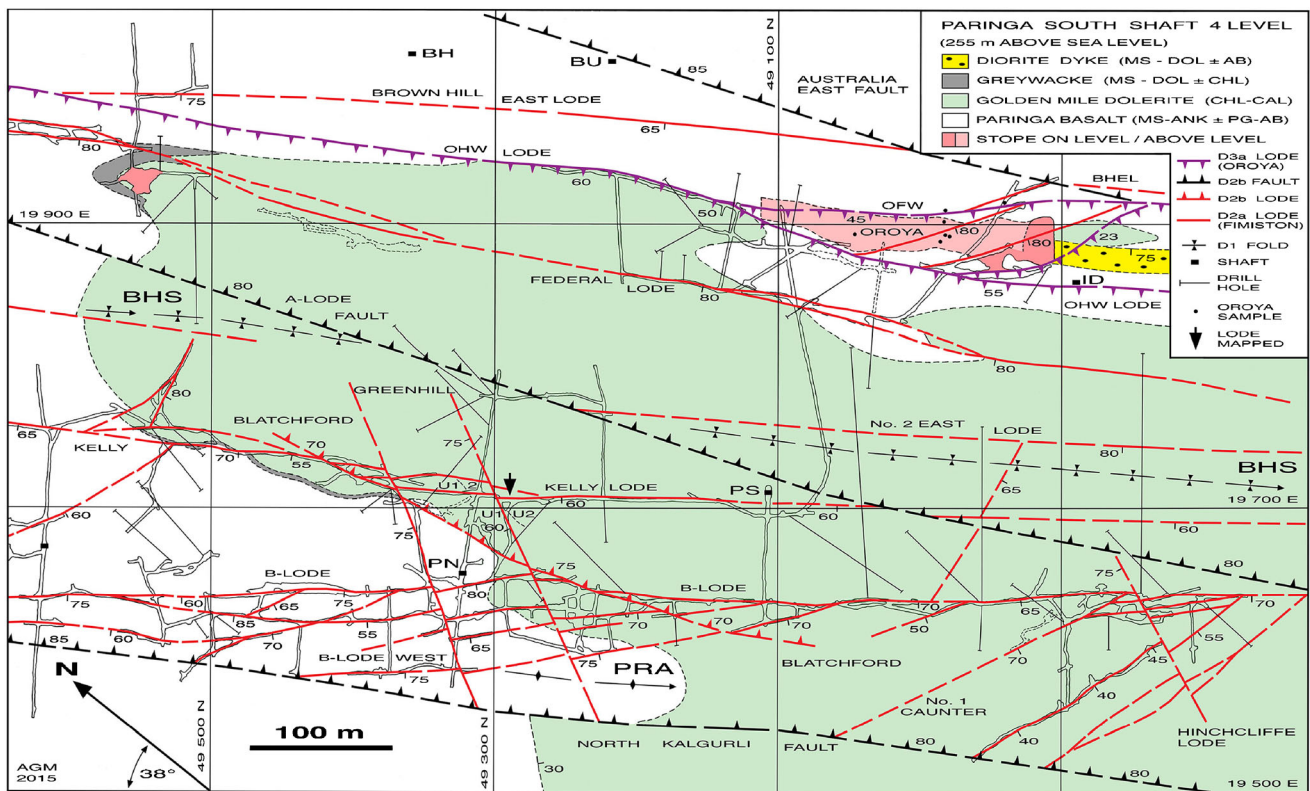
Fig. 8 Structural map of the Paringa South shaft 4 level, 255 m above sea level (166 m below datum), constructed using the 1:1000 mine survey plan, scattered historic geological data, gold assay data and the results of own mapping. The structures are ordered according to the time of formation (D1 to D3), and not according to the time of gold mineralisation. The coordinates are mine grid. The Oroya Shoot stope is projected onto the level according to survey data in Lungan (1986), and is 25 m above the level at 49,110 m N. Note the location of detailed face mapping of the D2a Kelly Lode (*arrow*). D1 folds: Brownhill Syncline (BHS), Paringa Anticline (PRA). D2/D3 lodes: D2a Brownhill East (BHEL), D3a Oroya Footwall (OFW), D3a Oroya Hanging Wall (OHW). Shafts: Brownhill (BH), Brownhill Underlay (BU), Iron Duke-Associated Northern (ID), Paringa North (PN), Paringa South (PS). Minerals: albite (ab), ankerite (ank), calcite (cal), chlorite (chl), dolomite (dol), muscovite (ms), paragonite (pg)
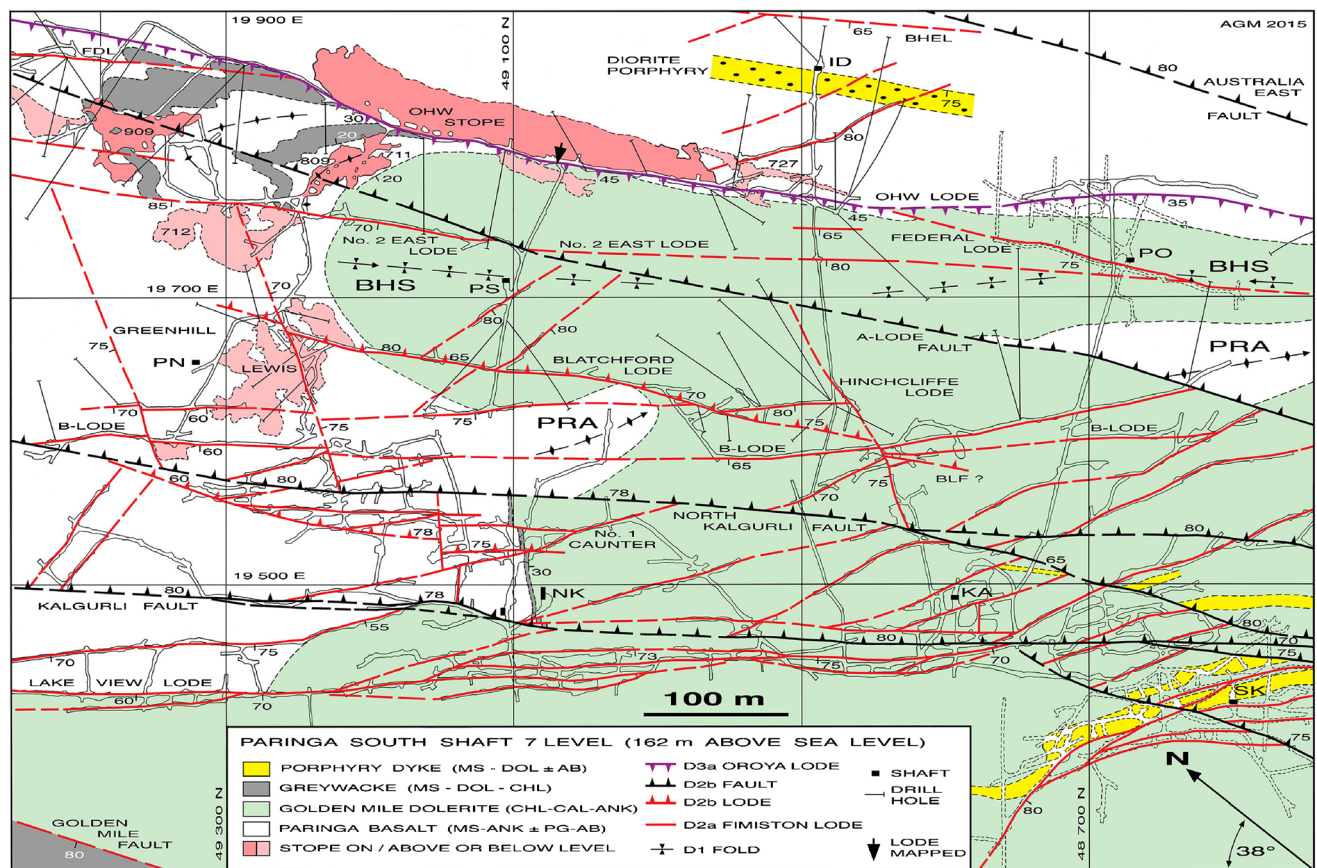
Fig. 9 Structural map of the Paringa South shaft 7 level (162 m above sea level) and of the North Kalgurli shaft 6 level (+165 m), constructed using the combined 1:1000 mine survey plan, scattered historic geological data, gold assay data and the results of own mapping. The projected workings (*dashed line*) of the other shafts are 7–17 m above or 9 m below the Paringa South 7 level. The structures are ordered according to the time of formation (D1 to D3), and not according to the time of gold mineralisation. The coordinates are mine grid. Note the location of

detailed face mapping of the D3a Oroya Hanging Wall (OHW) Lode. D1 folds: Brownhill Syncline (BHS), Paringa Anticline (PRA). D2a lodes: Brownhill East (BHEL), Federal (FDL). Shafts: Iron Duke-Associated Northern (ID), Kalgurli (KL), North Kalgurli (NK), Paringa North (PN), Paringa South (PS), Pomeroy (PO), South Kalgurli (SK). Minerals: albite (ab), ankerite (ank), calcite (cal), chlorite (chl), dolomite (dol), muscovite (ms), paragonite (pg)

thus oriented at higher angles of 55–65° relative to the average Main Lode (N40°W). The sense of movement has not been determined.

D2a Cross Lodes (R′ shear zones)

Two Cross Lodes termed Greenhill are exposed on the Paringa South 4 and 7 levels (Figs. 8 and 9). Both strike N25–30°E, the western lode dips 75°WNW, whereas the eastern one varies in dip from 70°WNW to 70°ESE. They displace the D2a Kelly Lode and B-Lode, and the D2b Blatchford Lode 2–7 m east block south, crosscutting relationships consistent with D2c reactivation. On level 4, the eastern lode consists of a laminated quartz-ankerite fault-fill vein at the footwall contact, and white-grey quartz-ankerite-pyrite replacement extending up to 50 cm into the hanging wall. The replacement zone

encloses angular fragments of GMD Unit 1 rimmed by comb-textured quartz. The D1 foliation in chlorite-calcite altered Golden Mile Dolerite is deformed indicating a dextral sense of movement (Fig. 11e). The eastern Greenhill Lode is crosscut in turn by a D3a quartz vein with 5–15 cm wide ankerite-pyrite selvages.

The Hinchcliffe Cross Lode strikes N20–25°E, dips 70–90°WNW or ESE and has an undulating shape in cross section implying strike-slip. On levels 4 and 7 of the Paringa South shaft, the lode is stoped over a short distance where it crosses and displaces the B-Lode (Figs. 8 and 9). On level 11, the Hinchcliffe Lode is vertical and terminates at one of the D2a Federal Hanging Wall lodes with lateral drag attributed to D2c sinistral strike-slip movement (Fig. 12). In remnant ore pillars, the lode is about 2 m thick, massive and has sharp boundaries. The northwest trending, 65–75°SW dipping foliation in sericite-ankerite altered Paringa pillow basalt is deformed
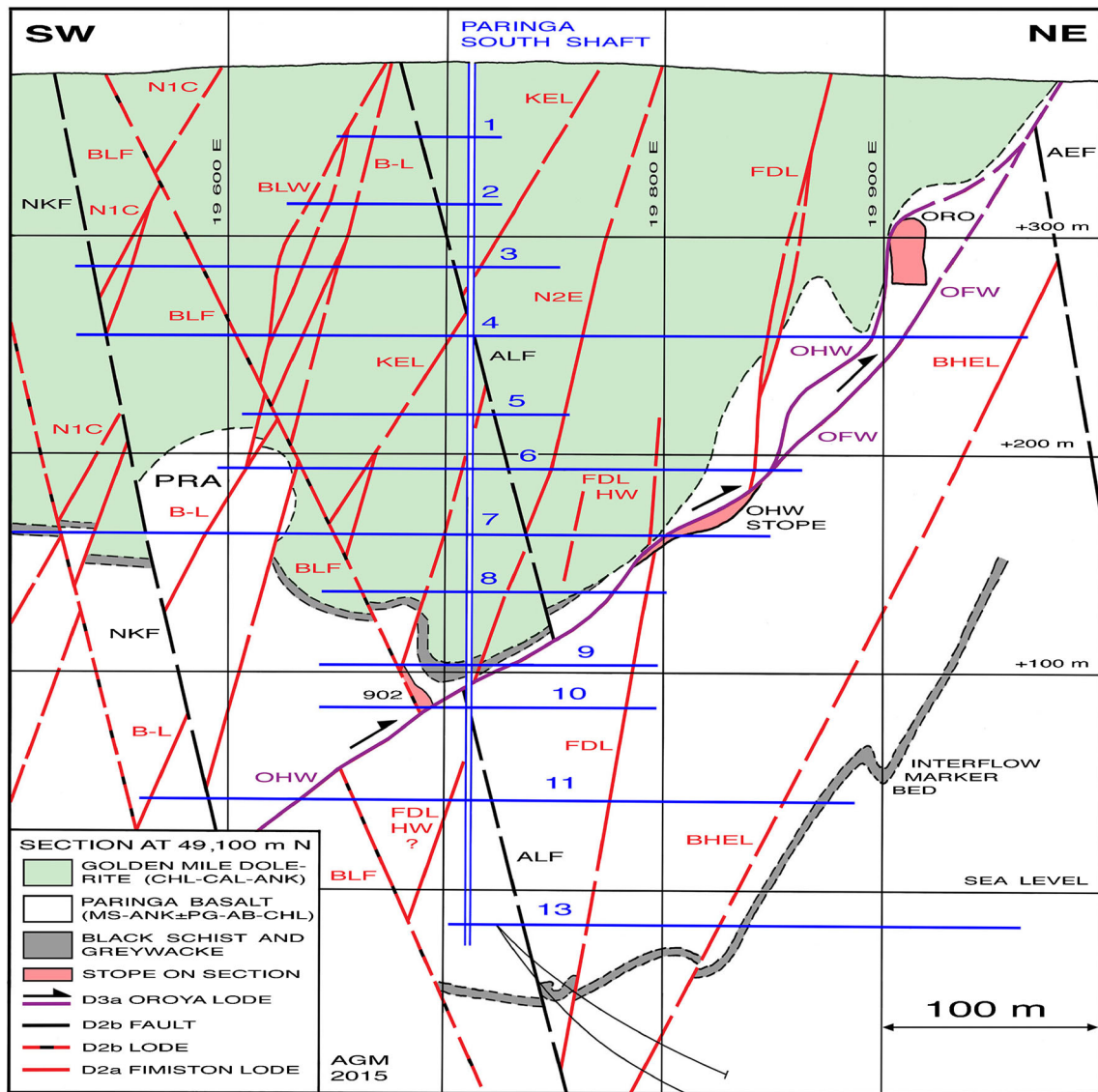
Fig. 10 Cross section through the D1 Brownhill Syncline at the Paringa South shaft at 49,100 m grid north, constructed using the results of own structural mapping on levels 4, 7 and 11 of the shaft, reconnaissance mapping on other levels and limited gold assay data. The carbonaceous greywacke lining the contact Golden Mile Dolerite-Paringa Basalt is shown schematically. A marker bed of black schist separates the lower magnesian from the upper tholeiitic Paringa Basalt (Tomich 1959). The structures are ordered according to the time of formation (D1 to D3), and not according to the time of gold mineralisation. D1 folds: Paringa Anticline (PRA). D2a lodes: B-Lode (B-L), B-Lode West (BLW), Brownhill East (BHEL), Federal (FDL), Federal Hanging Wall (FDL HW), Kelly (KEL), No. 1 Caunter (N1C), No. 2 East (N2E). D2b lodes: Blatchford (BLF). D2b faults: Australia East (AEF), A-Lode (ALF), North Kalgurli (NKF). D3a lodes: Oroya Footwall (OFW), Oroya Hanging Wall (OHW). Stopes: Oroya (ORO; after Lungan 1986), Oroya Hanging Wall (OHW), Blatchford (902). Minerals: albite (ab), ankerite (ank), calcite (cal), chlorite (chl), muscovite (ms), paragonite (pg)

defining a dextral structure identical to the one at the Greenhill Lode. The Hinchcliffe Lode crosscuts the D2b Blatchford Lode and, as indicated on stope plans, also crosses the D2b North Kalgurli Fault with little offset (Fig. 12).

D2b Australia East-type faults and lodes

The A-Lode Fault (N20°W/80°E) on the Paringa South shaft 7 level consists of a 5–15 cm thick chlorite-calcite-quartz S-C mylonite. Reverse movement on this fault

uplifted sericite-ankerite altered basalt of the Paringa Anticline into chloritic Golden Mile Dolerite (Fig. 9). The North Kalgurli Fault and the Kalgurli Fault, both oriented N30–35°W/80°NE, are represented by two closely spaced branches of 5-cm-thick barren S-C mylonite on the North Kalgurli shaft 11 level. Both cut across the D1 foliation (N40°W/70–80°SW) in chloritic Golden Mile Dolerite. The North Kalgurli Fault offsets the D2a shear zone of the B-Lode about 50 m in a reverse sense (Fig. 10), and the Kalgurli Fault displaces stratigraphic
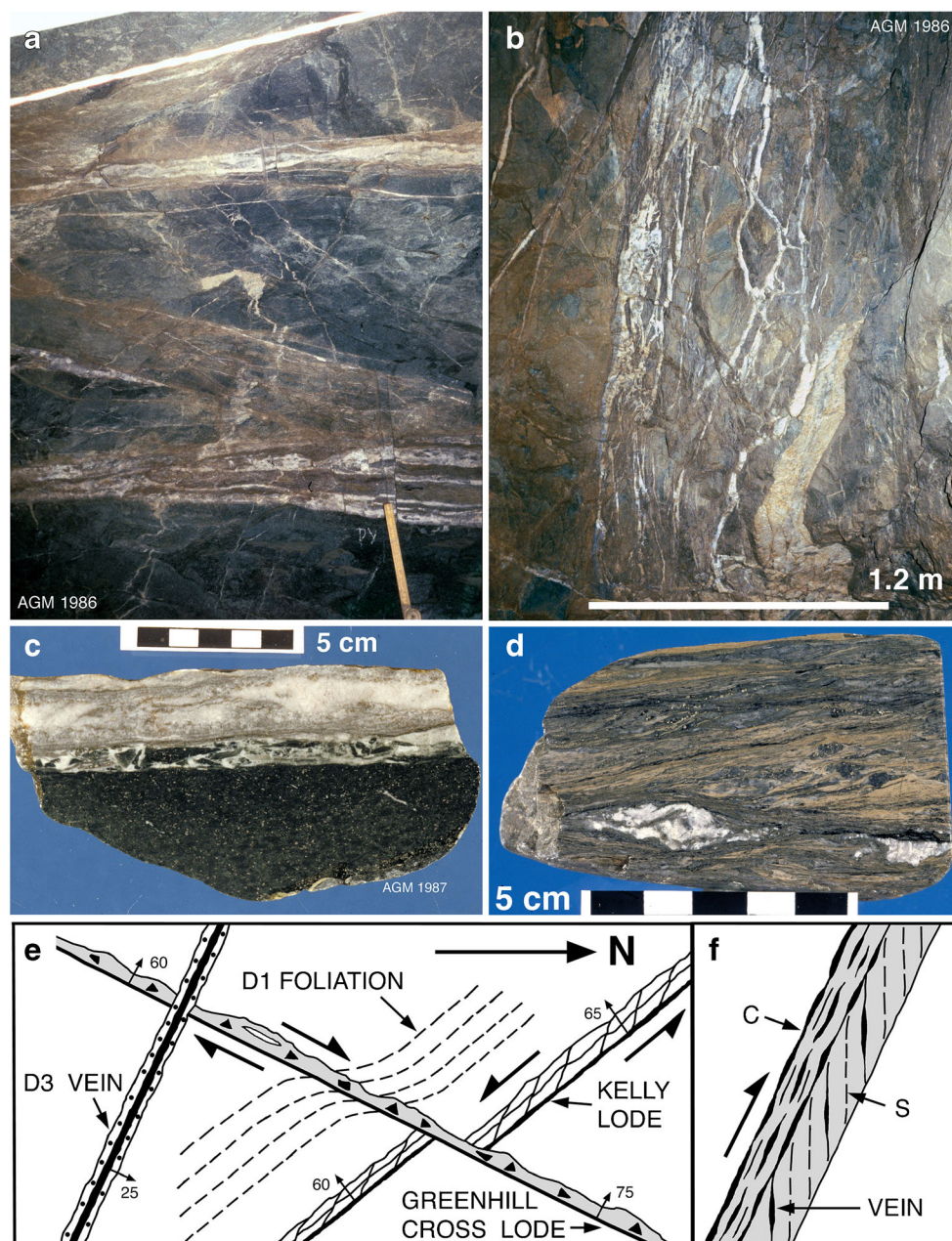
Fig. 11 Syn-mineralisation deformation textures (D2c and D3a) in reactivated D2a Fimiston and D2b Australia East-type shear zones representing gold ore (lodes), Paringa South mine, Golden Mile, Kalgoorlie. **a** D2a Kelly Lode, 4 level (49,280 m N): looking northeast at D2c quartz-dolomite-albite fault-fill veins with muscovite-ankerite-pyrite selvages (*brown*) replacing chlorite-calcite altered Golden Mile Dolerite (GMD) Unit 2. The scale is 30 cm long. **b** D2a Kelly Lode, 4 level (49,305 m N): looking N35°W at a cross section in a rise to the stope above, white D2c quartz-dolomite-albite veins in muscovite-ankerite-pyrite altered GMD Unit 2 enclosing remnant chloritic domains. **c** D2a Kelly Lode, 4 level: D2c fault-fill vein at the footwall contact composed of granular quartz, Fe-dolomite and pyrite. The parallel breccia vein encloses fragments of chloritic GMD Unit 2 cemented by Fe-calcite. **d** D2b Blatchford Lode, 11 level (49,000 m N): D2c/D3a muscovite-quartz-ankerite S-C mylonite with pinch-and-swell veins and seams of auriferous pyrite and tourmaline, main shear zone cutting across sericite-ankerite altered, barren Paringa pillow basalt. **e** D1 to D3 structures in the 4 level crosscut (49,290 m N) linking the Kelly and B-Lode (plan not to scale): the D1 foliation in chlorite-calcite altered Golden Mile Dolerite is dragged at the Greenhill Cross Lode (D2a), composed of a footwall fault-fill vein and a 50-cm-thick quartz-dolomite breccia (both D2c), which offsets the D2a Kelly Lode 2–3 m in a dextral sense. A D3a extension vein with ankerite-pyrite selvages cuts across the Greenhill Lode. **f** D2b Blatchford Lode, 11 level (49,030 m N): looking southeast at a cross section of the main shear zone, 15 cm thick, dipping 65°NE. The chlorite-muscovite-ankerite-pyrite mylonite overprints barren, sericite-ankerite altered Paringa pillow basalt. The geometry of the S-C fabric indicates reverse D3a movement

contacts, granodiorite dykes and D2a shear zones 175 m east side up (Gauthier et al. 2004).

On the Paringa South shaft 11 level, a telluride extension vein marked by comb-textured central quartz occurs adjacent
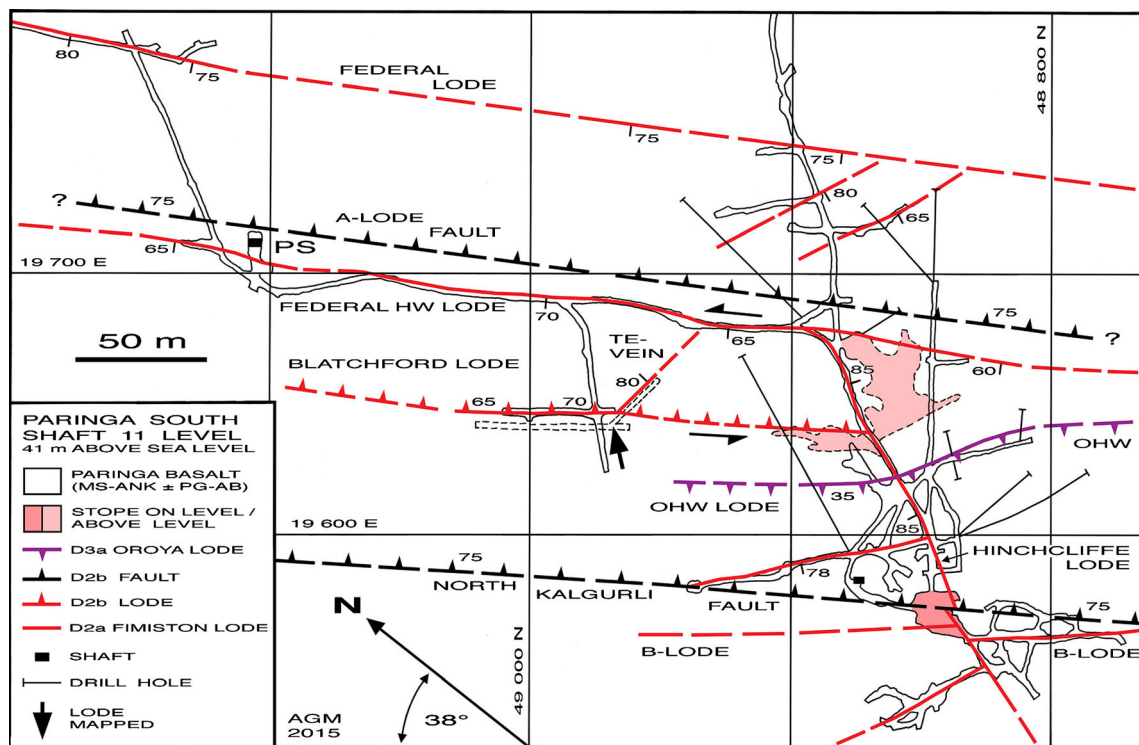
Fig. 12 Structural map of the Paringa South shaft 11 level, 41 m above sea level (380 m below datum), constructed using the 1:1000 mine survey plan, scattered historic geological data, gold assay data and the results of own mapping. The coordinates are mine grid. The structures are ordered according to the time of formation (D2a to D3a), and not according to the time of gold mineralisation. Note the location of detailed face mapping of the D2b Blatchford Lode (BLF) and telluride-bearing extension vein (TE-VEIN) in the sublevel 10 m above. The D2a Hinchcliffe Cross Lode terminates and displays left-lateral drag at the D2a Federal Hanging Wall Lode but crosscuts the D2b Blatchford Lode indicating D2c reactivation. The vertical Cross Lode shows no offset at the reverse D3a Oroya Hanging Wall (OHW) Lode. Shaft: Paringa South (PS). Minerals: albite (ab), ankerite (ank), muscovite (ms), paragonite (pg)

to the east dipping Blatchford Lode in sericite-ankerite altered Paringa pillow basalt (Fig. 12). The Blatchford Lode (N35°W/ 65–70°NE) is composed of a footwall S-C mylonite 3–15 cm thick (Fig. 11d), breccia lenses and a 0.5-m-wide fracture zone traced by fault-fill veins. Muscovite crenulations on C-planes striking perpendicular to the dip direction and the S-C geometry of the mylonite in cross section (Fig. 11f) indicate a reverse component of movement synchronous with mineralisation (D3a). The orientation of the telluride extension vein, in contrast, requires almost pure D2c strike-slip on the Blatchford Lode (Fig. 13a). The vein strikes 45° anticlockwise relative to the bounding shear zones, the classic orientation of an extensional Riedel T-structure formed during sinistral strike-slip, an interpretation consistent with the drag on the Hinchcliffe Cross Lode (Fig. 12).

Another east dipping D2b lode is exposed in crosscuts close to the North Kalgurli shaft at about 19,530 m east (Fig. 9). On level 12 of the shaft, this lode (N25°W/75°NE) consists of three zones of S-C mylonite 5–15 cm thick stoped over a width of 1.0–1.5 m. The mylonite zones contain tellurides, and the stope averaged up to 800 g/t gold in 1987. The host rock between the mylonites, sericite-ankerite altered Paringa pillow basalt, is crosscut by breccia veins and

mineralised with disseminated pyrrhotite. A telluride-bearing extensional shear vein (north/45°E) in the footwall of the lode suggests an east-west oriented maximum principal stress, an orientation implying D3a reverse sinistral oblique-slip on the main shear zone (Fig. 13a). Striations on slickenside shear planes pitch 20–25°SE, however, and indicate a late phase of D2c strike-slip.

D3a Oroya Hanging Wall Lode

The principal D3a shear zone in the Golden Mile is the Oroya Hanging Wall (OHW) Lode, which follows the Golden Mile Dolerite contact at the northeast limb of the D1 Brownhill Syncline replacing Paringa Basalt. In the Paringa South underground workings, the lode is exposed over a strike length of about 800 m (Figs. 8 and 9). In the high wall of the open pit, it is traced as a continuous fault surface down to the sea level (Fig. 14a), and underground exposures at the South Kalgurli shaft indicate down-dip continuity to at least 195 m below sea level (Fig. 4a). The OHW Lode displaces the D2a Federal Lode, the D2b Blatchford Lode and D2b A-Lode Fault 50 m southwest side up (Fig. 10). The strike varies from N25°W to N35°W, and the dip from 35° to 60°SW. Above the Paringa
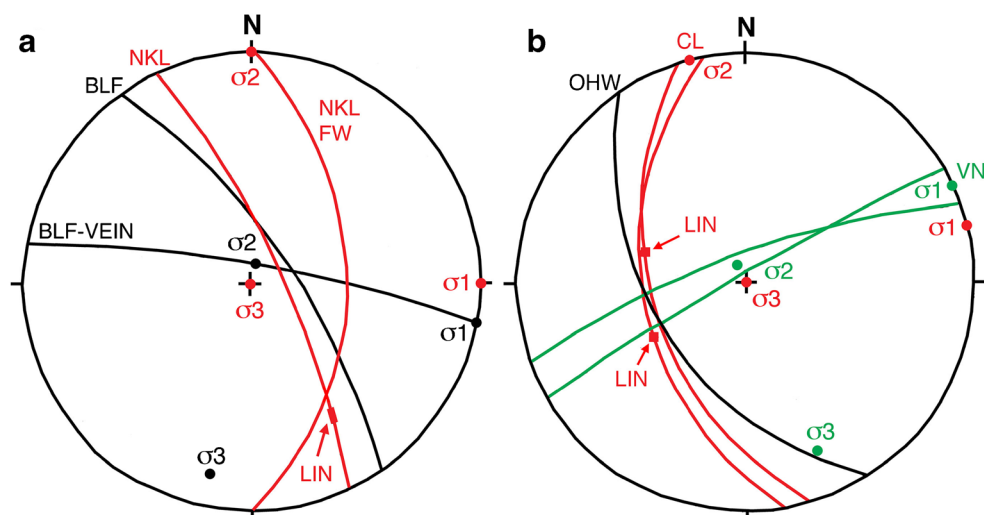
Fig. 13 Lower hemisphere equal-angle stereographic projections of syn-mineralisation D2c and D3a structures in reactivated D2b faults and in the D3a Oroya Hanging Wall (OHW) Lode, Paringa South and North Kalgurli mines, Golden Mile, Kalgoorlie. **a** In *black*, the D2b Blatchford Lode (BLF), Paringa South 11 level: the gold-telluride extension vein (BLF-VEIN) strikes 45° anticlockwise relative to the boundary sinistral shear zones (Fig. 12). Assuming extension perpendicular to the vein walls, the local stress regime is σ3 = 10° towards 190°, σ2 = 80° towards 10° and σ1 = 0° towards 100° parallel to the strike of the vein, consistent with D2c strike-slip on the bounding shear zones. In *red*, another D2b shear zone, North Kalgurli 12 level: a telluride-bearing shear zone (NKL) is connected to an extensional fault-fill vein of shallower dip in the footwall (NKL-FW). Assuming maximum principal stress perpendicular to strike of the footwall vein, the stress regime is σ1 = 0° towards 90°, σ2 = 0° north and σ3 is vertical. This

regime suggests D3a sinistral oblique-slip with a dominant reverse component on the main shear zone but striations (LIN, 20–25°SSE) record late D2c strike-slip. **b** D3a OHW Lode, Paringa South 7 level crosscut: the hanging wall boundary (OHW) of the reverse shear zone is controlled by the Golden Mile Dolerite-Paringa Basalt contact, the fracture cleavage (CL) in the lode is rotated clockwise in strike but maintains the same dip, striations (LIN) on cleavage planes pitch 65°NNW to 75°SSE. Gold-bearing extension veins (VN) strike perpendicular to the lode boundary. Assuming that the maximum principal stress is perpendicular to the average strike of the cleavage, the stress regime is σ1 = 0° towards 76°, σ2 = 0° towards 346° and σ3 is vertical. Assuming extension perpendicular to the vein walls, the stress regime is σ3 = 10° towards 155°, σ2 = 80° towards 335° and σ1 = 0° towards 65° parallel to the average strike of the veins. Both regimes are consistent with syn-mineralisation D3a ENE-WSW shortening

South 6 level, the lode splits into a hanging wall (OHW) and a footwall branch (OFW) close to the Iron Duke shaft (Figs. 8 and 10).

In contrast to the syn-mineralisation strike-slip (D2c) and/or reverse oblique-slip (D3a) reactivation of the pre-mineralisation D2a and D2b shear-zone network, the reverse OHW Lode formed entirely during mineralisation. On the Paringa South shaft 7 level, the lode is 1–2 m thick, high-grade (50 g/t Au) and consists of silica-pyrite, pyrite-siderite-chlorite and silica-ankerite-telluride replacement bands overprinting sericite-ankerite altered Paringa Basalt (Fig. 14b). The internal structure varies from laminated S-C mylonite to matrix-supported breccia. The upper shear-zone boundary at the GMD contact strikes N33°W/45°SW. The lode contains muscovite- and chlorite-plated cleavage planes parallel in dip but rotated 16–23° clockwise in strike, and marked by striations pitching 65°NNW to 75°SSE. Gold-bearing extension veins link the walls of the lode and strike N60–70°E/75–85°N, an orientation consistent with ENE-WSW bulk shortening (Fig. 13b). The stope on level 7 is up to 5 m high because of crackle and extension veins mined several metres into the footwall (Fig. 14b).

On the Paringa South 6 level, the OHW stope is only 0.7 m high. The lode consists of silica-pyrite and pyrite-siderite-

chlorite bands concentrated in replacement zones along the hanging wall and footwall boundaries. These zones are dominated by C-fabrics, and by boudinaged and drag-folded quartz-ankerite veins indicating reverse movement (Fig. 14c). Bleached Paringa Basalt is preserved in the centre overprinted by an oblique S-fabric. Remnant pillows are flattened and stretched in the S-fabric plane (Fig. 14d). About 100 m north of the stope, a 30-cm-thick dyke of chlorite-dolomite altered kersantite crosscuts sericite-ankerite altered Paringa Basalt and terminates in the OHW Lode (Mueller et al. 1988). The dyke strikes N65°E/85°NW, and is sub-parallel to mineralised extension veins (N60°E/80°NW) linking the OHW and OFW lodes at higher mine levels (Lungan 1986). On the lower shear boundary of the OHW Lode, the dyke is crosscut by barren extension veins oriented perpendicular to striations pitching 70°SE. The veins lack pyrite selvages where they traverse the dyke (Fig. 14e). Quartz-carbonate steps on the slickenside shear plane indicate southwest block up oblique-slip with a small dextral component (Fig. 14f). These structures indicate late to post-mineralisation reverse movement, probably before 2642 ± 6 Ma, the discordant zircon Pb-Pb age of the dyke (McNaughton et al. 2005). Although the above movement indicators are consistent with the 50 m reverse offset of D2a
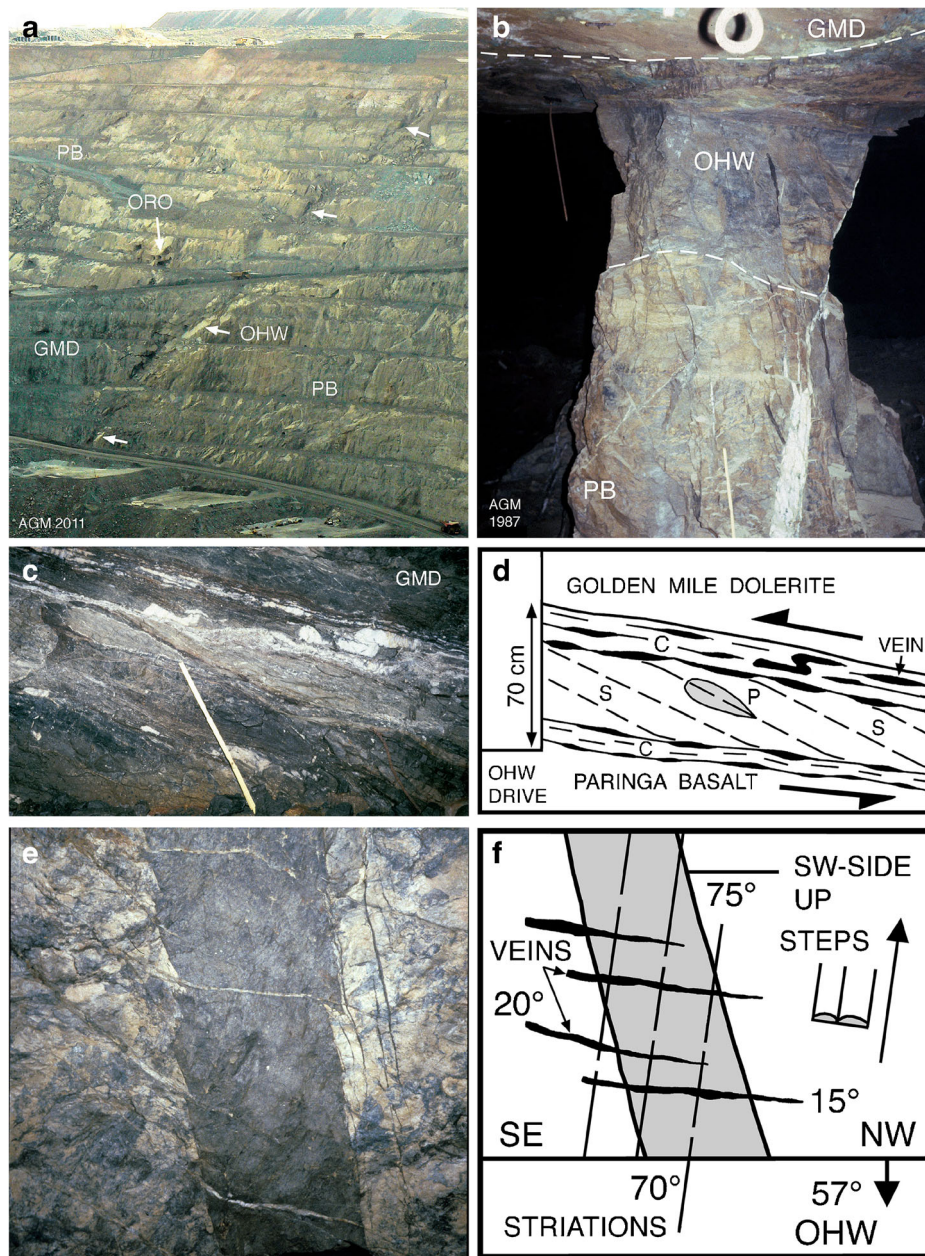
Fig. 14 Structure of the D3a Oroya Hanging Wall (OHW) Lode, open pit northeast wall and Paringa South shaft 6 and 7 levels, Golden Mile, Kalgoorlie. **a** Looking N30°W at the Paringa mine area in the open pit, visitor platform, April 2011. The OHW thrust fault (*arrows*) is traced from the surface to 260 m below at the haul road, mostly following the contact between chlorite-ankerite altered Golden Mile Dolerite (GMD) and sericite-ankerite altered Paringa Basalt (PB). The open stopes are part of the Oroya Shoot (ORO). The bench heights are 10–30 m. **b** OHW drive on 7 level at 49,070 m N/19,790 m E: looking N60°E at a pillar in the OHW stope, the yellow scale is 70 cm tall. Green chloritic GMD Unit 1 forms the roof, and is in contact with banded silica-pyrite and chlorite-siderite ore of the OHW shear zone (*dashed lines*). The white quartz-ankerite extension vein terminates in the shear zone and crosscuts sericite-ankerite altered Paringa pillow basalt (PB) and mineralised crackle veins. **c** OHW drive on 6 level at 49,230 m N/19,880 m E: looking southeast at a cross section of the OHW Lode, the yellow scale is 60 cm tall. Chlorite-ankerite altered GMD Unit 1 forms the upper boundary. Rusted silica-pyrite and pyrite-siderite-chlorite bands at both

shear boundaries replace sericite-ankerite altered Paringa Basalt (pillow *outlined by chalk*). The drag-folded white quartz-ankerite vein indicates reverse D3a movement. **d** OHW drive on 6 level: line drawing illustrating the structures in photograph **c**. The upper shear zone boundary dips 40°SW. C-fabric mylonite zones and foliation-parallel veins mark the hanging wall (20 cm) and footwall (10 cm). The S-fabric in the central sericite-ankerite schist dips 55–60°SW crossing flattened and stretched pillows (P). **e** OHW drive on 6 level at 49,315 m N/19,906 m E: looking southwest at the trace of the chlorite-dolomite altered kersantite dyke, 30 cm thick, on the lower muscovite-chlorite plated shear boundary of the OHW Lode. The white quartz-dolomite extension veins lack ankerite-pyrite alteration selvages in the dyke and are post-mineralisation (D3b). **f** OHW drive on 6 level: line drawing illustrating the structures in photograph **e**. Striations perpendicular to the trace of the extension veins pitch 70°SE on the OHW shear plane (dip 57°SW). Quartz-dolomite steps in the dyke formed when the southwest block moved up and northwest during reverse D3b oblique-slip

and D2b structures (Fig. 10), striations on some C-planes in the OHW Lode pitch 25°SE (Lungan 1986) suggesting intermittent minor strike-slip.

D3a Oroya Shoot

The reverse OHW shear zone controls the Oroya Shoot in the Paringa Basalt (62 t Au; Gustafson and Miller 1937), a pipe-shaped ore body unique in the Golden Mile due to its length (1.3 km) and shallow plunge (Fig. 15). From the outcrop to the Iron Duke shaft, the shoot plunges 14°SE and the OHW Lode forms the hanging wall boundary. Close to surface, the D2a Brownhill East Lode constitutes the footwall (Fig. 15). About 150 m southeast of the Iron Duke shaft, the OHW Lode crosses to the footwall of the shoot creating a gap in the stope. Further southeast, the shoot is located between the OHW Lode and the Golden Mile Dolerite close to the hinge of the Brownhill Syncline (Stillwell 1929).

A complex structural control exists between the Paringa South and Iron Duke shafts due to the local folding of the GMD-Paringa Basalt contact, and the branching of the Oroya shear system into the OHW and OFW lodes (Fig. 8), both connected by the flat Middle Fault described in Larcombe (1913). Further complexity is added by northwest striking, sericite-dolomite altered diorite dykes (see App. 2), and by crossing D2a Caunter Lodes (Figs. 8 and 16). The Caunter Lodes link the Brownhill East and Federal lodes but are displaced by the reverse D3a shear system (Fig. 16). The

oval cross section of the Oroya Shoot is due to the selective mining of pyrite-telluride mylonite ore, and of high-grade crackle-vein and breccia ore (120 g/t Au) at the intersection of the D3a shear zones.

D3a contact breccia lodes

Tabular breccia ore bodies (Lewis, 711, 712, 809, 909 stopes) occur in spatial association with altered carbonaceous schist and greywacke close to the GMD-Paringa Basalt contact at the closure of the Brownhill Syncline between levels 6 and 8 of the Paringa South shaft (Figs. 9 and 15). Like the lithologic contact, the ore bodies are of shallow dip (15–25°SW to SE). The D3a OHW Lode and adjacent D2a lodes form the lateral boundaries (Fig. 9). The Lewis ore body offsets the D2a Greenhill Cross Lodes 15 m hanging wall block northwest (Fig. 15). Striations on planes of the 711 ore body indicate dip-slip.

The ore bodies consist of quartz-sulphide veins in carbonaceous sericite-quartz schist, and foliated to massive breccia in sericite-ankerite altered Paringa Basalt. The fragments (1–5 cm, locally 10–20 cm) are cemented and variably replaced by pyrite (10–30 vol.%), silica, ankerite and chlorite. Tellurides are present locally (Scantlebury 1983). Most stopes are 2–5 m high but stope 909 extends 20 m downward into D2a shear zones of the Federal system.
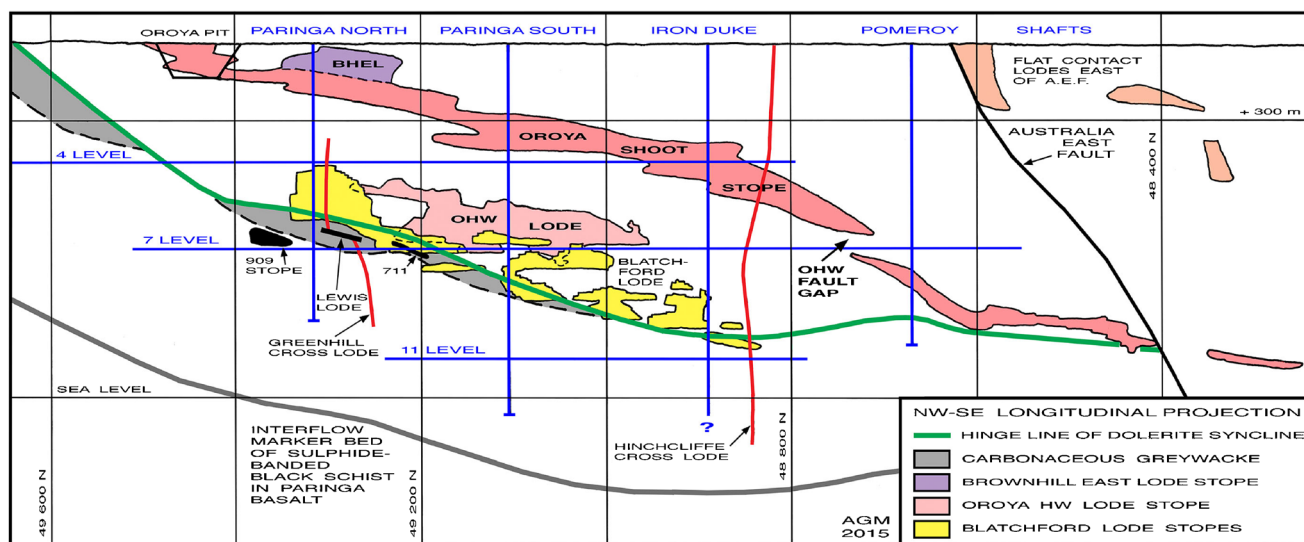
Fig. 15 Northwest-southeast longitudinal projection onto a vertical plane through the hinge of the D1 Brownhill Syncline (modified from Tomich 1959) showing the following stopes: D2b Blatchford Lode, D3a Oroya Hanging Wall (OHW) Lode, D3a Oroya Shoot (pre-1936; Gustafson and Miller 1937) and D3a breccia ore bodies at the contact Paringa Basalt-Golden Mile Dolerite. The D2a Greenhill and Hinchcliffe Cross Lodes are traced. The variable dip of the Hinchcliffe Lode about the vertical implies strike-slip movement. The Greenhill Lode is displaced at the D3a Lewis Lode. The Golden Mile Dolerite sill crosscuts carbonaceous greywacke along its contact with the Paringa Basalt. The marker bed of black schist separates lower magnesian from upper tholeiitic Paringa Basalt. The structures are ordered according to the time of formation (D1 to D3a), and not according to the time of gold mineralisation. The coordinates are metric mine grid
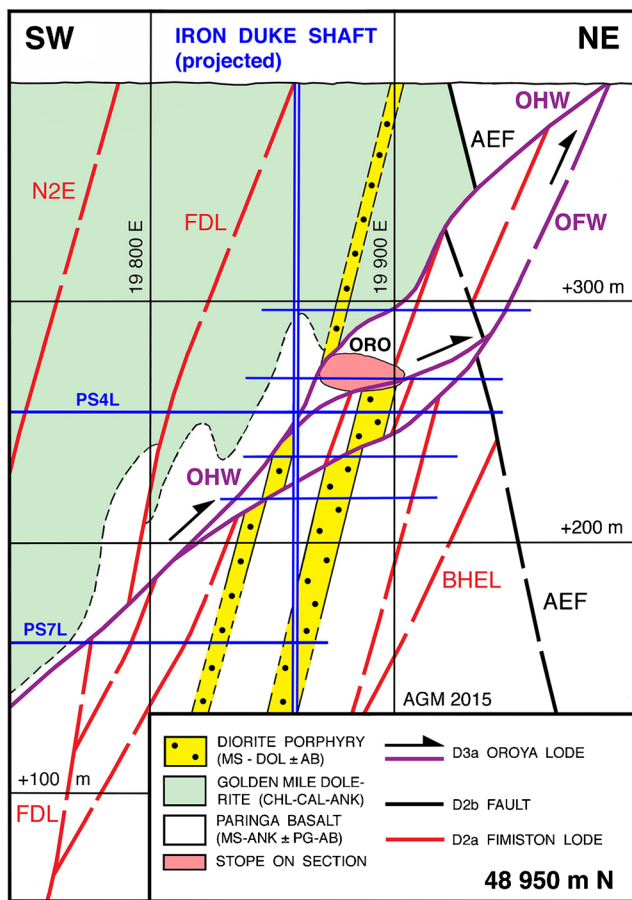
Fig. 16 Cross section at 48,950 m grid north through the northeast limb of the D1 Brownhill Syncline, the D3a Oroya shear-zone system and the Oroya Shoot (ORO) north of the Iron Duke shaft (projected from 48,890 m N), constructed using own data and cross sections in Larcombe (1913) and Stillwell (1929). The coordinates are metric mine grid. The structures are ordered according to the time of formation (D1 to D3a), and not according to the time of gold mineralisation. D2a Fimiston Lodes: Brownhill East (BHEL), Federal (FDL), No. 2 East (N2E). D2b faults: Australia East (AEF). D3a Oroya Lodes: Oroya Footwall (OFW), Oroya Hanging Wall (OHW). Minerals: albite (ab), ankerite (ank), calcite (cal), chlorite (chl), dolomite (dol), muscovite (ms), paragonite (pg)

D3a Blatchford Shoot

The Blatchford Shoot follows the hinge of the Brownhill Syncline further down plunge than the contact ore bodies maintaining the spatial association with carbonaceous, sericite-dolomite altered greywacke (Fig. 15). The shoot consists of pipe-shaped ore bodies 20–30 m long and 4 × 6 m in cross section located in Paringa Basalt above the intersection of the Blatchford and OHW Lodes (902 stope in Fig. 10). The "ore pipes" are connected to narrow (1 m) stopes on the Blatchford shear zone in Golden Mile Dolerite above. In the 902 stope, pyrite-rich quartz-ankerite-chlorite breccia is cross-cut by N85°W striking, sub-vertical extension veins up to 50 cm thick and more than 20 m long, which connect the Blatchford and one of the Federal Hanging Wall Lodes, a structural setting replicated on level 11 below (Fig. 12).

Barren east-west faults (post-D3)

On the Paringa South 4 level (49,270 m N), a barren fault (N85°E/85°S) marked by a 2-cm-thick chlorite-calcite S-C mylonite offsets the D2a Kelly Lode 1 m south block down causing normal drag on the mineralised veins. On the Paringa South 6 level (49,310 m N), a narrow barren fault oriented N75°E/85°S offsets the D3a OHW Lode 1.5 m south block down. Lateral drag suggests a sinistral component of movement, and striations pitch 10–15°ENE on the fault plane. The faults postdate Fimiston- and Oroya-style mineralisation in the Paringa South mine, but their structural relationship to the D4 faults of the Golden Pike system is not constrained.

Discussion

The complexity of the Golden Mile lode system and the superposition of movement indicators due to fault reactivation delayed the understanding of its structural setting and evolution. Stillwell (1929) concluded that the local shear zones developed prior to the intrusion of the granodiorite dykes, and that they were reactivated during mineralisation after dyke emplacement. Gustafson and Miller (1937) recognised the presence of regional folds. They reasoned that the geometry of the lode pattern on both limbs of the Kalgoorlie Syncline precludes a relationship to folding, and supported Stillwell's conclusion that the porphyry dykes were emplaced prior to mineralisation. Campbell (1953) suggested lode formation during regional faulting in conjunction with folding, and postulated dextral southwest side down displacement on the Golden Mile Fault. Woodall (1965) and Clout et al. (1990) interpreted the lodes as shear zones subsidiary to the dextral Golden Pike and Adelaide Faults. Phillips (1986) and Boulter et al. (1987) proposed that they formed during regional folding as ductile shear zones in response to the infiltration of an auriferous metamorphic fluid. Mueller and Harris (1987) and Mueller et al. (1988) concluded that the Golden Mile lodes are related to post-folding sinistral shearing on the regional Boulder Lefroy and Golden Mile faults, and that the quartz-vein ore bodies at Mt. Charlotte are related to younger dextral faulting. Bateman et al. (2001b) proposed that the Fimiston Lodes formed during early recumbent folding and west directed thrusting on the Golden Mile Fault, and that the mineralised fault system was rotated into its present upright position during a second phase of folding. Gauthier et al. (2007) disputed this interpretation pointing to the consistent strike and dip of porphyry dykes across the Kalgoorlie Anticline and Syncline. Recently, the discussion has turned to the craton-scale tectonic setting, whether the Golden Mile formed in a fold belt at a convergent plate-tectonic margin (e.g. Czarnota et al. 2010; Witt et al. 2017; this issue) or during the inversion of an intra-cratonic

rift (e.g. Barnes et al. 2012). The structural evolution of the Golden Mile deposit with time, concisely summarised in Fig. 17, is discussed below based on the evidence presented in this study.

Pre-mineral formation of D2a shear zones

Regional D1 folding during ENE-WSW bulk shortening took place after the emplacement of the Golden Mile Dolerite sill at 2685 ± 5 Ma (Tripp 2013). A weak axial-plane foliation (S1) defined by actinolite-albite assemblages developed in the mafic units of the Kalgoorlie Anticline and Syncline during burial metamorphism at 400 MPa lithostatic pressure, equivalent to 14 km crustal depth (3.6 km/100 MPa; e.g. Bucher and Frey 2002). The D2a Boulder Lefroy and Golden Mile faults displace the D1 folds. In response to stress generated during kilometre-scale strike-slip on these master faults, extensive systems of D2a shear zones formed in Golden Mile Dolerite and Paringa Basalt, both competent metamorphic rocks of high-iron tholeiitic composition. The shear zones developed prior to the emplacement of granodiorite porphyry dykes into the Golden Mile system at 2674 ± 6 Ma, and into the Boulder Lefroy Fault at 2676 ± 7 Ma (Kent and McDougall 1995;

Mueller et al. 2016; this issue). The emplacement of granodiorite dykes took place after peak D1 metamorphism but prior to gold mineralisation.

**Geometry of D2a shear zones in the Golden Mile**

The contoured density lower hemisphere projections of D2a shear zones traced by Fimiston Lodes in the Perseverance and Paringa South mines illustrate an organised network (Fig. 18). As recognised by Gustafson and Miller (1937), the absence of mirror-image geometry on both sides of the Kalgoorlie Syncline precludes pure shear during D1 folding as a viable mechanism. If the peak of greenschist-facies metamorphism coincided with D1 folding, as indicated by the S1 axial-plane foliation, then the formation of the D2a shear zones as "fault-fracture meshes" in coherent rocks will be problematic due to the passing of the high-pressure fluid conditions required (Sibson 2000). The time constraints imposed by the granodiorite dykes also suggest that the flux of metamorphic fluid preceded the infiltration of the hydrothermal fluid generating the deposit. Geometric analysis differs from the fluid-induced stress-field analysis of Sibson (2000) by referencing the shear zone orientations to the D2a Golden Mile master fault. The
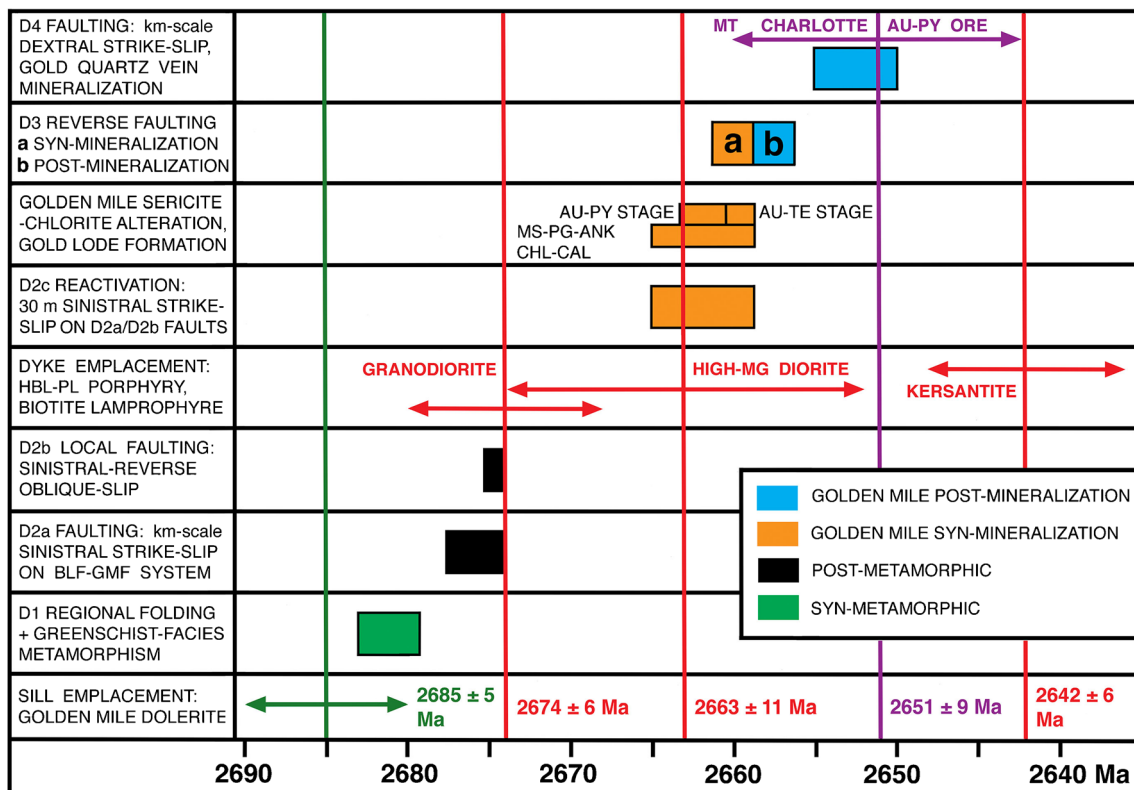
Fig. 17 Time line diagram linking wall-rock alteration, gold-pyrite-telluride mineralisation and the deformation events (D1 to D4) in the Golden Mile to the U-Pb ages imposed by the local porphyry dykes (zircon) and by the Mt. Charlotte gold ore (xenotime). The discordant zircon Pb-Pb age of the kersantite dyke is interpreted as a minimum constraint. Abbreviations: Boulder Lefroy Fault (BLF), Golden Mile Fault (GMF), Fimiston gold-pyrite mineralisation (Au-py stage), Oroya gold-telluride mineralisation (Au-Te stage). Minerals: ankerite (ank), calcite (cal), chlorite (chl), hornblende (hbl), muscovite (ms), paragonite (pg), plagioclase (pl). The U-Pb ages (±2 sigma errors) are from Kent and McDougall (1995), McNaughton et al. (2005), Gauthier et al. (2007), Tripp (2013) and Mueller et al. (2016; this issue)
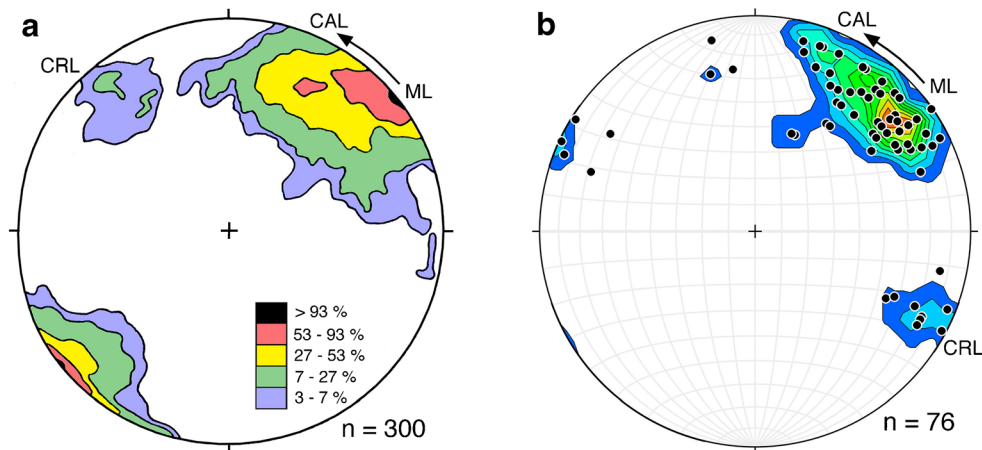
Fig. 18 Lower hemisphere equal-area projections showing the contoured density of the poles to D2a shear zones traced by Fimiston Main Lodes (ML), Caunter Lodes (CAL) and Cross Lodes (CRL) in principal displacement, Riedel and conjugate Riedel orientation, respectively. Extensional Riedel shears (R + T) trend towards shallower dips and greater anticlockwise strike angles relative to the Main Lodes. **a**

Perseverance shaft 3 level (131 m below datum), percentage counts relative to the maximum in a 1% area, lodes surveyed during underground development, modified from Ion (1982). **b** Paringa South shaft 3 to 11 levels and North Kalgurli shaft 6 level, 2% contour intervals of density in a 1% area, projection generated using Stereonet 9.3.3 of Cardozo and Allmendinger (2013)

results indicate that the Fimiston Lodes trace two sinistral Riedel shear systems (Mueller et al. 1988).

Shear fractures generated by bulk simple shear were first modelled in clay-cake experiments (e.g. Riedel 1929; Tschalenko 1970), and then mapped after earthquakes in poorly consolidated sediments above strike-slip basement faults (e.g. Tschalenko and Ambraseys 1970). Other field-based studies reviewed in Sylvester (1988) and in Davis et al. (2012) have shown that Riedel shears also form as large-scale systems in homogenous competent rocks such as the Navajo Sandstone without any relationship to a basement fault (Davis et al. 2000).

The orientation and sense of movement of Fimiston Lodes in the Paringa South mine closely match those of shear fractures in sinistral strike-slip zones (Table 2). Most Caunter Lodes correspond to Riedel shears. Others represent hybrids combining Riedel (R) and extension (T) segments, a geometry

caused by step-wise propagation at the tip of Riedel shears (Sylvester 1988). Conjugate Riedel (R′) shears such as the Greenhill and Hinchcliffe Cross Lodes are less common and display evidence of selective reactivation (discussed below). The Horseshoe No. 3 and No. 4 Lodes in the Western Lode System and the Federal Lode in the Eastern System are interpreted as synthetic P shear zones. The B-Lode and the Lake View Lode represent braided principal displacement zones linked to adjacent Main Lodes by Riedel shears, hybrid R-T shears and T shear zones of normal displacement.

D2b Australia East-type faults

The Australia East-type faults, parallel in strike to D2a P-shear zones but dipping steeply east, are not part of the Riedel strike-slip systems. They also predate the emplacement of granodiorite porphyry dykes (Fig. 4a), and are thus older than

Table 2 Classification of D2a Fimiston Lodes according to strike angle relative to the Golden Mile Fault or the bounding Main Lode principal displacement zone, Paringa South mine, Golden Mile, Kalgoorlie

Golden Mile lode name	Average strike and dip	Strike angle to principal shear (average + range)	Empirical angle (Sylvester 1988)	Classification (Sylvester 1988)	Predominant movement
Main	N40°W/60–75°SW	Parallel (±5°)	0°	Principal zone	Sinistral strike-slip
Main	N30°W/±90°	+10° (+5 to +15°)	+15 to +20°	P shear	Sinistral strike-slip
Caunter	N60°W/60–70°SW	−23° (−15 to −30°)	−15 to −20°	Riedel shear (R)	Sinistral strike-slip
Caunter	N86°W/60–80°S	−40° (−36 to −48°)	−45°	Normal fault (T)	Normal?
Cross	N26°E/±90°	+66° (+60 to +74°)	+60 to +75°	Conjugate Riedel (R′)	Dextral strike-slip

Strike angles clockwise from the principal displacement zone are positive; anticlockwise ones are negative

2674 ± 6 Ma. The pre-mineralisation movement, as indicated by the offset of GMD units, was probably reverse oblique-slip moving the east side up and north. The preferential development of D2b faults within the D2a block containing the Kalgoorlie Anticline suggests that they formed late during sinistral faulting when movement to the northwest became restricted. The intermittent locking of the anticlinal fault block during kilometre-scale transport resulted in the arching of the D1 fold axis (Mueller et al. 1988), and in the refolding of the Golden Mile Fault against the Boulder Lefroy Fault northwest of the Kalgoorlie district (Mueller et al. 2016; this issue).

Timing of Golden Mile hydrothermal activity

Sericite-dolomite alteration overprints granodiorite porphyry dykes in sheared greywacke of the D2a Golden Mile Fault, and is thus younger than 2671 ± 10 Ma (Vielreicher et al. 2010), and sericite-ankerite alteration overprints diorite dykes in the kilometre-scale Paringa Basalt contact zone. The sericite zones are located within a wider chlorite zone caused by widespread fluid infiltration into the D2a/D2b fault and fracture system. Crosscutting relationships and magnetite-pyrite mineralised xenoliths in dykes (Gauthier et al. 2007) indicate that the Golden Mile hydrothermal event coincided broadly with the emplacement of diorite porphyries at 2663 ± 11 Ma (Fig. 17). The zircon U-Pb ages of high-Mg monzodiorite stocks 12 km southeast of the Golden Mile (2662 ± 6 to 2658 ± 3 Ma; Mueller 2007) and the xenotime U-Pb age of the D4 Mt. Charlotte gold quartz-vein ore (2651 ± 9 Ma; Mueller et al. 2016; this issue) support this interpretation. Given the large error (±11 Ma) of the single diorite age published (Gauthier et al. 2007), additional zircon chronology is required. It may be targeted at diorite dykes following transverse D2a shear zones (R'), and at those displaced by the reverse D3a faults of the Oroya system (Fig. 16). The dykes at the Oroya Shoot are overprinted by sericite-ankerite alteration of the Paringa Basalt contact zone (App. 2), which may thus be younger than ca. 2663 Ma. The early biotite alteration in porphyry intersected by drill hole SE-1 also needs further petrographic and chronologic study. The selective replacement of hornblende by biotite is characteristic of potassic alteration in porphyry deposits worldwide (e.g. Seedorff et al. 2005). The genesis of the kilometre-scale chloritoid-paragonite-ankerite zone southeast of the Golden Mile is discussed in Part 2 of the Paringa South study (this issue).

Syn-mineralisation D2c strike-slip faulting

In the Golden Mile, progressive hydrothermal alteration of the greenschist-facies tholeiitic rocks lowered the shearing resistance and reactivated pre-mineralisation D2a and D2b faults. Granodiorite and diorite porphyry dykes were displaced up to 30 m, a small amount compared to the kilometre-scale pre-

porphyry displacement of folded meta-gabbro sills (Mueller et al. 2016; this issue). The brittle fault-fill and extension veins, ductile S-C mylonites and the lineations in the lodes were generated during this phase of D2c faulting. The syn-mineralisation movement on D2a Main Lodes (e.g. Kelly, Federal) was sinistral strike-slip with a small southwest side down component, indicated by the offsets of stratigraphic contacts and by striations pitching 10–25°SE. Many D2b faults are also marked by striations of shallow pitch. Left-lateral movement on the D2b Blatchford Lode generated a sub-vertical telluride-rich extension vein. The geometric setting of the vein indicates that the maximum principal stress (σ1) during D2c strike-slip faulting was horizontal and oriented N100°E.

Syn-mineralisation D3a reverse faulting

The D3a OHW Lode offsets D2a and D2b shear zones 50 m in a reverse sense. Internal shear planes, lineations and extension veins indicate that the reverse movement took place during bulk shortening, when the maximum principal stress (σ1) was horizontal and oriented N65–76°E. The contact of the Golden Mile Dolerite at the southwest dipping limb of the Kalgoorlie Anticline, lined with lenses of carbonaceous greywacke, presented a weak surface favourable for reverse faulting leading to the formation of the OHW Lode and the Oroya Shoot. The breccia ore bodies at the closure of the D1 Brownhill Syncline exploit shallowly dipping surfaces formed by the Black Flag greywacke-GMD-Paringa Basalt contacts. They record metre-scale dip-slip and are interpreted as lateral escape thrusts taking up strain in the hanging wall of the OHW Lode during D3 shortening.

Reverse components of movement attributed to D3a are recorded on a few D2b faults of the Australia East system, most notably on the North Kalgurli telluride lode, where geometric relations indicate a maximum principal stress oriented N90°E. However, striations pitching 20–25°SE on planes of this lode and 25°SE on those of the D3a OHW Lode indicate late strike-slip. These contradictory structural relationships are interpreted to result from alternating periods of syn-mineralisation D2c strike-slip and D3a reverse faulting. Conjugate Riedel shears such as the Greenhill Cross Lodes also moved during this D2/D3 transition, as they displace other D2a and the D2b lodes by several metres. Cross Lodes striking N20–25°E were in a favourable orientation for dextral reactivation during D3a when the maximum principal stress rotated to N65°E, the direction indicated by extension veins in the OHW Lode. Two phases of syn-mineralisation movement are also recorded in the D2a Golden Mile Fault at Mt. Charlotte: reverse sinistral oblique-slip moving the northeast block up and northwest along a line pitching

60°SE and late sinistral strike-slip indicated by offsets at telluride-bearing fault-fill veins (Mueller 2015).

Post-mineralisation D3b reverse faulting

Post-mineralisation D3 shortening generated the barren D3b reverse faults in the Western Lode System, and formed the sericite foliation (S2) of constant orientation in Fimiston Lodes of different strike described in Boulter et al. (1987), perhaps by propagation and enhancement of the S1 axial-plane foliation. Protracted ENE-WSW shortening also caused the buckling of auriferous veins oriented at a high angle to S2 (Gauthier et al. 2004).

D4 mineralisation postdating the Golden Mile system

The barren D3b thrusts in the Western Lode System, where D4 gold quartz veins of the Drysdale ore body overprint the D2a Horseshoe No. 2 Lode (Clout et al. 1990), indicate a gap in time between the D2c/D3a Golden Mile and the D4 hydrothermal systems. The dextral strike-slip faults formed in response to a rotation of the maximum principal stress to a NE-SW direction. D4 reactivation of earlier faults took place adjacent to the Golden Pike Fault, and affected mainly D2b faults of similar strike. All D4 gold ore bodies including the Aberdare Lodes and the quartz-vein stockworks (Figs. 1 and 2) consist of sericite-ankerite-pyrite mineralisation without telluride ore. The xenotime U-Pb age of 2651 ± 9 Ma for the Mt. Charlotte deposit (Mueller et al. 2016; this issue) is the most precise constraint on mineralisation during D4 strike-slip faulting (Fig. 17).

Conclusions

(1) The D2a and D2b shear zones traced by the Fimiston Lodes in the Golden Mile were generated after D1 regional folding and burial metamorphism, when kilometre-scale sinistral strike-slip on the bounding Boulder Lefroy and Golden Mile master faults strained greenschist-facies, tholeiitic GMD and Paringa Basalt. Riedel, conjugate Riedel, P shear zones and principal displacement shear zones formed in these metamorphic rocks on both sides of the northwest striking Golden Mile Fault. Granodiorite porphyry dykes were emplaced at 2674 ± 6 Ma into the D2 shear system after peak D1 metamorphism but prior to hydrothermal activity.

(2) Hydrothermal fluid infiltrated and reactivated the D2a/D2b sinistral fault system during the emplacement of diorite porphyry dykes at 2663 ± 11 Ma. Chlorite-calcite ± ankerite alteration developed in an area 5 km long and more than 1 km wide enclosing two zones of pre-sulphide sericite-ankerite alteration, one centred on

the Golden Mile Fault and the other on the folded GMD-Paringa Basalt contact. Intermittent D2c sinistral strike-slip took place from early Fimiston gold-pyrite to late Oroya gold-telluride mineralisation during post-porphyry faulting (≤30 m displacement).

(3) The D2c strike-slip faulting alternated with periods of D3a reverse faulting during ENE-WSW bulk shortening, which generated the OHW Lode and the shallowly plunging Oroya Shoot, both high grade (30–120 g/t Au) and rich in tellurides. The D2c and D3a regimes alternated until D3 shortening prevailed and barren D3b reverse faults offset the Fimiston Lodes southwest of the Golden Mile Fault.

(4) North striking D4 strike-slip faults displaced the D2/D3 shear-zone system up to 2 km in a dextral sense generating Mt. Charlotte-style gold quartz-vein ore bodies at 2651 ± 9 Ma. D4 veins overprint D2a Fimiston Lodes and barren D3b thrusts in the Golden Mile. The D4 ore bodies are characterised by sericite-ankerite-pyrite replacement in chlorite-altered GMD, lack telluride ore and represent resurgent hydrothermal systems postdating the Golden Mile system.

The superposition of mineralised D2 to D4 structures in the Golden Mile was caused by changes in the orientation of the far-field maximum stress from its predominant ENE-WSW direction during D1 and D3, first to the southeast during sinistral transcurrent faulting (D2) and later to the northeast during dextral faulting (D4). Such a dynamic stress regime is more compatible with a plate-tectonic convergent margin than an intra-cratonic rift setting, and may be caused by periods of orthogonal and oblique subduction. A similar history is recorded at the arc-parallel Domeyko Fault in the Andes of Chile, where transcurrent faults crossing the Eocene-Oligocene Chuqui porphyry complex changed from early dextral to late sinistral strike-slip of 35 km left-lateral displacement (Ossandón et al. 2001).

References

Baker G (1958) Tellurides and selenides in the Phantom Lodes, Great Boulder mine, Kalgoorlie. Australasian Inst Min Metall, Melbourne, Stillwell Ann. Vol., pp 15–40

Barnes SJ, van Kranendonk MJ, Sonntag I (2012) Geochemistry and tectonic setting of basalts from the Eastern Goldfields Superterrane. Aust J Earth Sci 59:707–735

Bartram GD, McCall GJH (1971) Wall-rock alteration associated with auriferous lodes in the Golden Mile, Kalgoorlie. In: Glover JE (ed) Symposium on Archaean rocks. Geol Soc Australia, Publication 3, pp 191–199

Bateman R, Costa S, Swe T, Lambert D (2001a) Archaean mafic magmatism in the Kalgoorlie area of the Yilgarn Craton, Western Australia: a geochemical and Nd isotopic study of the petrogenetic and tectonic evolution of a greenstone belt. Precambrian Res 108: 75–112

Bateman RJ, Hagemann SG, McCuaig TC, Swager CP (2001b) Protracted gold mineralization throughout Archaean orogenesis in the Kalgoorlie camp, Yilgarn Craton, Western Australia: structural, mineralogical, and geochemical evolution. Geol Survey Western Australia, Record 2001/17, pp 63–98

Beyschlag F, Vogt JHL, Krusch P (1916) The deposits of the useful minerals and rocks (vol. 2, translated from German by SJ Truscott). MacMillan, London, pp 590–598

Boulter CA, Fotios MG, Phillips GN (1987) The Golden Mile, Kalgoorlie: a giant deposit localized in ductile shear zones by structurally induced infiltration of an auriferous metamorphic fluid. Econ Geol 82:1661–1678

Bucher K, Frey M (2002) Petrogenesis of metamorphic rocks, 7th edn. Springer, Berlin, 341 pp

Campbell JD (1953) The structure of the Kalgoorlie Goldfield. In: Edwards AB (ed) Geology of Australian ore deposits. 5th Empire Min Metall Congress, Melbourne, pp 79–93

Cardozo N, Allmendinger RW (2013) Spherical projections with OS-X Stereonet. Comput Geosci 51:193–205

Clout JMF, Cleghorn JH, Eaton PC (1990) Geology of the Kalgoorlie goldfield. In: Hughes FE (ed) Geology of the mineral deposits of Australia and Papua New Guinea. Australasian Inst Min Metall, Monograph 14, Melbourne, pp 411–431

Czarnota K, Champion DC, Goscombe B, Blewett RS, Cassidy KF, Henson PA, Groenewald PB (2010) Geodynamics of the eastern Yilgarn Craton. Precambrian Res 183:175–202

Davis GH, Bump AP, García PE, Ahlgren SG (2000) Conjugate Riedel deformation band shear zones. J Struct Geol 22:169–190

Davis GH, Reynolds JR, Kluth CF (2012) Structural geology of rocks and regions, 3rd edn. Wiley, New York, 839 pp

Feldtmann FR (1928) Interim report on the geology and ore deposits of Kalgoorlie. Geol Survey Western Australia, Annual Report for 1927, pp 16–30

Finucane KJ (1941) East-dipping strike faults on the Boulder Belt, Kalgoorlie. Proc Aust Inst Min Metall 124:203–215

Finucane KJ (1948) Ore distribution and lode structures in the Kalgoorlie goldfield. Proc Aust Inst Min Metall 148:111–129

Finucane KJ (1964) Ore penetration into calc schist on the Kalgoorlie goldfield. Proc Aust Inst Min Metall 211:49–59

Finucane KJ, Jensen HE (1953) Lode structures in the Kalgoorlie gold-field. In: Edwards AB (ed) Geology of Australian ore deposits. Aust Inst Min Metall, Melbourne, pp 94–111

Fletcher IR, Dunphy JM, Cassidy KF, Champion DC (2001) Compilation of SHRIMP U-Pb geochronological data, Yilgarn Craton, Western Australia, 2000–2001. Geoscience Australia, Record 2001/47, 111 pp

Fotios MG (1983) Structural analysis of mineralized shear zones in the Lake View and Perseverance gold mines, Kalgoorlie. B.Sc. (Honours) thesis, the University of Western Australia, Perth

Gauthier L (2006) Atlas of Fimiston-style mineralisation paragenesis, Golden Mile gold deposit, Kalgoorlie, W.A. Centre for Exploration Targeting, the University of Western Australia, Perth

Gauthier L, Hagemann S, Robert F, Pickens G (2004) Structural architecture and relative timing of Fimiston gold mineralization in the Golden Mile deposit, Kalgoorlie. Geol Survey Western Australia, Record 2004/16, pp 53–60

Gauthier L, Hagemann S, Robert F (2007) The geological setting of the Golden Mile gold deposit, Kalgoorlie, WA. In: Bierlein FP, Knox-Robinson CM (eds) Kalgoorlie 2007, Old Ground, New Knowledge, Abstracts. Geoscience Australia, Record 2007/14, pp 181–185

Goscombe BD, Blewett RS (2009) Plate 1: East Yilgarn Craton metamorphism and strain map. Geoscience Australia Map Series: http://www.ga.gov.au/data-pubs/maps

Gustafson JK, Miller FS (1937) Kalgoorlie geology re-interpreted. Proc Aust Inst Min Metall 106:93–125

Hagemann SG, Cassidy KF (2000) Archean orogenic lode gold deposits. SEG Rev 13:9–68

Ion JC (1982) Wallrock alteration and structural evolution of steeply dipping Golden Mile dolerite hosted lodes of the Perseverance gold mine, Kalgoorlie. B.Sc. (Honours) thesis, the University of Western Australia, Perth

Keats W (1987) Regional geology of the Kalgoorlie-Boulder gold-mining district. Geol Survey Western Australia, Report 21, 44 pp

Kent AJR, McDougall I (1995) ^{40}Ar-^{39}Ar and U-Pb age constraints on the timing of gold mineralization in the Kalgoorlie gold field, Western Australia. Econ Geol 90:845–859

Larcombe COG (1913) The geology of Kalgoorlie, Western Australia, with special reference to the ore deposits. Australasian Inst Min Engineers, Melbourne, Monograph, 315 pp

Lee RF (1980) Simultaneous determination of carbon and sulphur in geological material using inductive combustion. Chem Geol 31: 145–151

Lister GS, Snoke AW (1984) S-C mylonites. J Struct Geol 6:617–638

Lungan A (1986) The structural controls of the Oroya Shoot: implications for the structure of the Kalgoorlie region, Western Australia. B.Sc. (Honours) thesis, the University of Western Australia, Perth

McNaughton NJ, Mueller AG, Groves DI (2005) The age of the giant Golden Mile deposit, Kalgoorlie, Western Australia: ion-microprobe zircon and monazite U-Pb geochronology of a synmineralization lamprophyre dike. Econ Geol 100:1427–1440

Meyer C, Hemley JJ (1967) Wall rock alteration. In: Barnes HL (ed) Geochemistry of hydrothermal ore deposits, 1st edn. Holt, Rinehart and Winston, New York, pp 166–235

Mikucki EJ, Roberts FI (2004) Metamorphic petrography of the Kalgoorlie region, Eastern Goldfields granite-greenstone terrane: METPET database. Geol Survey Western Australia, Record 2003/12, 40 pp

Mueller AG (2007) Copper-gold endoskarns and high-Mg monzodiorite-tonalite intrusions at Mt. Shea, Kalgoorlie, Australia: implications for the origin of gold-pyrite-tennantite mineralization in the Golden Mile. Mineral Deposita 42:737–769

Mueller AG (2015) Structure, alteration, and geochemistry of the Charlotte quartz vein stockwork, Mt. Charlotte gold mine, Kalgoorlie, Australia: time constraints, down-plunge zonation, and fluid source. Mineral Deposita 50:221–244

Mueller AG, Harris LB (1987) An application of wrench tectonic models to mineralized structures in the Golden Mile district, Kalgoorlie, Western Australia. In: Ho SE, Groves DI (eds) Recent advances in understanding Precambrian gold deposits. University of Western Australia, geology department and university extension, publication 11, pp 97–107

Mueller AG, Harris LB, Lungan A (1988) Structural control of greenstone-hosted gold mineralization by transcurrent shearing—a new interpretation of the Kalgoorlie mining district, Western Australia. Ore Geol Rev 3:359–387

Mueller AG, Hagemann SG, McNaughton NJ (2016) Neoarchean orogenic, magmatic and hydrothermal events in the Kalgoorlie-

Kambalda area, Western Australia: constraints on gold mineralization in the Boulder Lefroy-Golden Mile fault system. Mineral Deposita. doi:10.1007/s00126-016-0665-9

Nelson DR (1997) Evolution of the Archaean granite-greenstone terranes of the eastern Goldfields, Western Australia: SHRIMP U-Pb zircon constraints. Precambrian Res 83:57–81

Nixon D (2015) Kalgoorlie Core Library drill hole report, sampling approval K627 and K636-K649, drill holes SE1-SE15 from the South End of Golden Mile, Fimiston, Kalgoorlie, Western Australia. Geological Survey of Western Australia, WAMEX Report 106097, 72 pp

Norrish K, Hutton JT (1969) An accurate X-ray spectrographic method for the analysis of a wide range of geological samples. Geochim Cosmochim Acta 33:431–453

O'Beirne WR (1968) The acid porphyries and porphyroid rocks of the Kalgoorlie area. Dissertation, the University of Western Australia, Perth, 410 pp

Ossandón G, Fréraut R, Gustafson LB, Lindsay DD, Zentilli M (2001) Geology of the Chuquicamata mine: a progress report. Econ Geol 96:249–270

Phillips GN (1986) Geology and alteration in the Golden Mile, Kalgoorlie. Econ Geol 81:779–808

Prider RT (1947) Chloritoid at Kalgoorlie. Am Mineral 32:471–474

Rasmussen B, Mueller AG, Fletcher IR (2009) Zirconolite and xenotime U-Pb constraints on the emplacement of the Golden Mile Dolerite sill and gold mineralization at the Mt. Charlotte mine, eastern Goldfields Province, Yilgarn Craton, Western Australia. Contrib Mineral Petrol 157:559–572

Riedel W (1929) Zur Mechanik geologischer Brucherscheinungen. Centralblatt Mineralogie und Paläontologie 1929(B):354–368

Robert F, Poulsen KH (2001) Vein formation and deformation in greenstone gold deposits. Rev Econ Geol 14:111–155

Scantlebury GM (1983) The characterization and origin of the gold lodes in and around the Brownhill Syncline, Golden Mile, Kalgoorlie, Western Australia. B.Sc. (Honours) thesis, the University of Western Australia, Perth, 90 pp

Seedorff E, Dilles JH, Proffett JM Jr, Einaudi MT, Zurcher L, Stavast WJA, Johnson DA, Barton MD (2005) Porphyry deposits: characteristics and origin of hypogene features. Econ Geol 100th Anniversary Volume, pp 251–298

Sibson RH (2000) A brittle failure mode plot defining conditions for high-flux flow. Econ Geol 95:41–47

Simpson ES (1930) Contributions to the mineralogy of Western Australia. J Royal Soc Western Australia 16:25–30

Stillwell FL (1929) Geology and ore deposits of the Boulder Belt, Kalgoorlie. Geol Survey Western Australia, Bulletin 94, 110 pp

Swager CP, Griffin TJ, Witt WK, Wyche S, Ahmat AL, Hunter WM, McGoldrick PJ (1995) Geology of the Archaean Kalgoorlie terrane—an explanatory note: Geol Survey Western Australia, Report 48, 26 pp

Sylvester AG (1988) Strike-slip faults. Geol Soc Am Bull 100:1666–1703

Thomson JA (1913) On the petrology of the Kalgoorlie goldfield, Western Australia. Q J Geol Soc London 69:621–677

Tomich SA (1952) Some structural aspects of Kalgoorlie geology. Proc Aust Inst Min Metall 164/165:45–76

Tomich SA (1959) The Oroya Shoot and its relationship to other flatly plunging ore pipes at Kalgoorlie. Proc Aust Inst Min Metall 190:113–124

Travis GA, Woodall R, Bartram GD (1971) The geology of the Kalgoorlie Goldfield. In: Glover JE (ed) Symposium on Archaean Rocks. Geol Soc Australia, Pub 3, pp 175–190

Tripp G I (2013) Stratigraphy and structure in the Neoarchaean of the Kalgoorlie district, Australia: Critical controls on greenstone-hosted gold deposits. Dissertation, James Cook University, Townsville, 475 pp

Tschalenko JS (1970) Similarities between shear zones of different magnitudes. Geol Soc Am Bull 81:1625–1640

Tschalenko JS, Ambraseys NN (1970) Structural analysis of the Dasht-e Bayaz (Iran) earthquake fractures. Geol Soc Am Bull 81:41–60

Vielreicher NM, Groves DI, Snee LW, Fletcher IR, McNaughton NJ (2010) Broad synchroneity of three gold mineralization styles in the Kalgoorlie goldfield: SHRIMP U-Pb and ^{40}Ar-^{39}Ar geochronological evidence. Econ Geol 105:187–227

Wells AA (1964) Western lode structures and southwards extensions of the Boulder mining belt. Proc Aust Inst Min Metall 211:181–192

Winchester JA, Floyd PA (1977) Geochemical discrimination of different magma series and their differentiation products using immobile elements. Chem Geol 20:325–343

Witt WK, Cassidy KF, Lu Y-J, Hagemann SG (2017) The tectonic setting and evolution of the 2.7 Ga Kalgoorlie-Kurnalpi Rift, a world-class Archean gold province. Miner Deposita, in press

Woodall R (1965) Structure of the Kalgoorlie goldfield. 8th Commonwealth Mining and Metallurgy Congress, Melbourne, pp 71–79

Yeats CJ, McNaughton NJ, Ruettger D, Bateman R, Groves DI, Harris JL, Kohler E (1999) Evidence for diachronous Archean lode gold mineralization in the Yilgarn Craton, Western Australia: a SHRIMP U-Pb study of intrusive rocks. Econ Geol 94:1259–1276